

See discussions, stats, and author profiles for this publication at: <https://www.researchgate.net/publication/21701185>

# Eklund, H. et al. Structure of oxidized bacteriophage T4 glutaredoxin (thioredoxin): refinement of native and mutant proteins. J. Mol. Biol. 228, 596–618

ARTICLE *in* JOURNAL OF MOLECULAR BIOLOGY · DECEMBER 1992

Impact Factor: 4.33 · DOI: 10.1016/0022-2836(92)90844-A · Source: PubMed

---

CITATIONS

72

READS

36

---

## 9 AUTHORS, INCLUDING:



Pär Nordlund

Karolinska Institutet

180 PUBLICATIONS 9,379 CITATIONS

[SEE PROFILE](#)



Matti Nikkola

Karolinska Institutet

17 PUBLICATIONS 584 CITATIONS

[SEE PROFILE](#)

## Structure of Oxidized Bacteriophage T4 Glutaredoxin (Thioredoxin)

### Refinement of Native and Mutant Proteins

Hans Eklund, Margareta Ingelman, Bengt-Olof Söderberg, Tomas Uhlin  
Pär Nordlund, Matti Nikkola, Ulf Sonnerstam, Thorleif Joelson

Department of Molecular Biology  
Swedish University of Agricultural Sciences  
Biomedical Center, Box 590, S-751 24 Uppsala, Sweden

and Kyriacos Petratos†  
EMBL Outstation, c/o Desy, D2000 Hamburg 52, Germany

(Received 23 March 1992; accepted 10 July 1992)

The structure of wild-type bacteriophage T4 glutaredoxin (earlier called thioredoxin) in its oxidized form has been refined in a monoclinic crystal form at 2·0 Å resolution to a crystallographic *R*-factor of 0·209. A mutant T4 glutaredoxin gives orthorhombic crystals of better quality. The structure of this mutant has been solved by molecular replacement methods and refined at 1·45 Å to an *R*-value of 0·175. In this mutant glutaredoxin, the active site residues Val15 and Tyr16 have been substituted by Gly and Pro, respectively, to mimic that of *Escherichia coli* thioredoxin.

The main-chain conformation of the wild-type protein is similar in the two independently determined molecules in the asymmetric unit of the monoclinic crystals. On the other hand, side-chain conformations differ considerably between the two molecules due to heterologous packing interactions in the crystals. The structure of the mutant protein is very similar to the wild-type protein, except at mutated positions and at parts involved in crystal contacts.

The active site disulfide bridge between Cys14 and Cys17 is located at the first turn of helix  $\alpha$ 1. The torsion angles of these residues are similar to those of *Escherichia coli* thioredoxin. The torsion angle around the S–S bond is smaller than that normally observed for disulfides: 58°, 67° and 67° for wild-type glutaredoxin molecule A and B and mutant glutaredoxin, respectively. Each sulfur atom of the disulfide cysteines in T4 glutaredoxin forms a hydrogen bond to one main-chain nitrogen atom.

The active site is shielded from solvent on one side by the  $\beta$ -carbon atoms of the cysteine residues plus side-chains of residues 7, 9, 21 and 33. From the opposite side, there is a cleft where the sulfur atom of Cys14 is accessible and can be attacked by a nucleophilic thiolate ion in the initial step of the reduction reaction.

**Keywords:** glutaredoxin; thioredoxin; refinement; redox active cysteines; mutant protein

### 1. Introduction

Thioredoxin and glutaredoxin are small proteins that take part in a variety of redox reactions in the cell (Holmgren, 1985, 1989). The thioredoxin of *Escherichia coli* was originally isolated and identified as being responsible for the reduction of disulfides essential for the activity of ribonucleotide reductase (Laurent *et al.*, 1964). Many alternative

roles for thioredoxins have later been suggested (see Holmgren, 1985, 1989). Thioredoxins have been shown to be involved in other metabolic pathways such as sulfate reduction (Black *et al.*, 1960) and as regulators of cell processes, particularly in plants (Cséke & Buchanan, 1986). The enzyme thioredoxin reductase regenerates reduced thioredoxin from the oxidized form.

A related redox protein was subsequently found in *E. coli*. The protein was termed glutaredoxin since it is reduced by glutathione and not by thioredoxin reductase. Both of these proteins contain redox-active cysteine residues but have very low

† Present address: Institute of Molecular Biology and Biotechnology, P.O. Box 1527, GR-711 10 Heraklion-Crete, Greece.

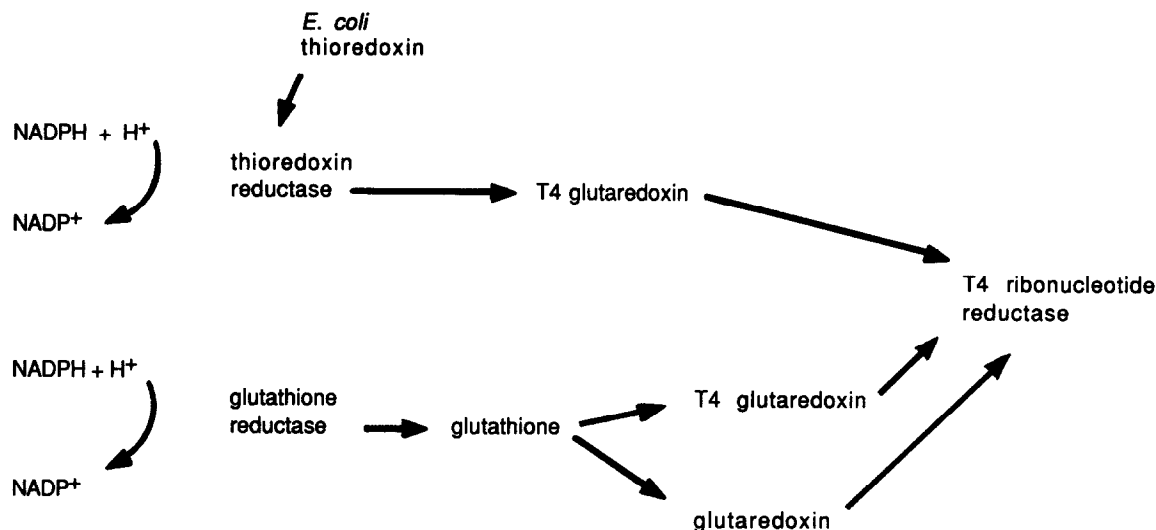


**Figure 1.** Bacteriophage T4 ribonucleotide reductase reduces ribonucleotides to deoxyribonucleotides in the infected cell. The reduction of ribonucleotide reductase can occur *via* at least 2 pathways. T4 glutaredoxin is a hybrid molecule that can use both the thioredoxin (top) and glutaredoxin pathways (bottom) for its reduction.

sequence homology except for the residues at the carboxyl end (Höög *et al.*, 1983). However, model building of the glutaredoxin indicates a similar fold for the two proteins (Eklund *et al.*, 1984). This has recently been proven to be correct by a nuclear magnetic resonance (n.m.r.†) structure determination (Sodano *et al.*, 1991).

Bacteriophage T4 carries a gene for a redox active cysteine containing protein involved in the synthesis of precursors for DNA synthesis (Berglund & Sjöberg, 1970). It reacts specifically with the bacteriophage T4 ribonucleotide reductase. It can be reduced by thioredoxin reductase and then serve in the reduction of ribonucleotides for viral DNA synthesis. Later, this protein was shown to be active also as a glutaredoxin (Holmgren, 1978). Because of its similarity in activity to *E. coli* thioredoxin, the T4 protein was originally called a thioredoxin since glutaredoxins were unknown at that time.

Thioredoxin sequences from different species form a homogeneous group with approximately the same chain length of about 107 residues. They contain conserved residues along the sequence including the active site sequence Trp-Cys-Gly-Pro-Cys (see Eklund *et al.*, 1991). Glutaredoxins form a more divergent group with more variation in chain length and with a different pattern of conserved residues (see Nikkola *et al.*, 1991). Sequence comparisons show that the redox protein of phage T4 has the characteristic pattern of conserved residues for glutaredoxins and should thus be called T4 glutaredoxin (Eklund *et al.*, 1984; Nikkola *et al.*, 1991).

T4 glutaredoxin is thus a functional hybrid of thioredoxin and glutaredoxin and can be reduced by either thioredoxin reductase or glutathione (Holmgren, 1978). In view of its properties, T4

glutaredoxin can be regarded as a glutaredoxin that has acquired properties to enable recruitment of the thioredoxin reductase system. The T4 glutaredoxin can then better use the reducing power of the bacterial cell for the production of viral DNA precursors (Fig. 1). Phage T4 is not dependent upon its own glutaredoxin and ribonucleotide reductase, but together, these proteins have the ability to direct the synthesizing machinery of the host cell towards T4 propagation.

*E. coli* thioredoxin is the most studied of all thioredoxins. It contains 108 residues, and the three-dimensional structure of the oxidized protein was solved at 2.8 Å (1 Å = 0.1 nm) resolution (Holmgren *et al.*, 1975). The structure of this protein has been refined at 1.68 Å to an *R*-value of 16.5% (Katti *et al.*, 1990). Thioredoxin structures have recently been determined by n.m.r. (LeMaster & Richards, 1988; Dyson *et al.*, 1990; Forman-Kay *et al.*, 1991).

The three-dimensional structure of T4 glutaredoxin was solved at 2.8 Å resolution with anomalous dispersion data from the native Cd-containing crystals and one heavy-atom derivative, Pt(NH<sub>3</sub>)<sub>2</sub>Cl<sub>2</sub>(*cis*) (Söderberg *et al.*, 1978). The Pt-atom binds to the sulfur atom of Met1 in both molecules, the only methionine which is fully exposed to solvent.

The three-dimensional structure is very similar for *E. coli* thioredoxin and T4 glutaredoxin in spite of the lack of sequence homology; 68 C<sup>α</sup> atoms (all residues excluding gaps) superimpose with a root-mean-square (r.m.s.) difference of 2.6 Å (Eklund *et al.*, 1984). The largest difference is the stretch of the first 20 residues in *E. coli* thioredoxin, which has no counterpart in T4 glutaredoxin.

A number of studies of T4 glutaredoxin have stimulated interest in the detailed structure of the molecule: site-directed mutagenesis (Joelson *et al.*, 1990; Nikkola *et al.*, 1991), studies of protein

† Abbreviations used: n.m.r., nuclear magnetic resonance; r.m.s., root-mean-square; Mes, 2-(*N*-morpholino)ethanesulfonic acid.

stability (Borden & Richards, 1990*a,b*), n.m.r. investigations (LeMaster & Richards, 1988) and molecular dynamics (Nilsson *et al.*, 1990; Nilsson, 1991). We have now completed refinement of the T4 glutaredoxin structure at 2·0 Å resolution. During the final stages of this work, we crystallized a mutant T4 glutaredoxin protein in a new crystal form with much improved diffraction (to at least 1·45 Å). We have solved this structure by molecular replacement methods and refined it. Since the information from both structures is complementary, we here report the refinement of both forms. In the mutant glutaredoxin, the residues between the redox-active cysteines were changed from Val-Tyr in the wild-type protein to Gly-Pro. The latter is the conserved sequence in the corresponding positions in thioredoxins (see Eklund *et al.*, 1991). This mutant protein will in this paper be referred to simply as "the mutant T4 glutaredoxin".

## 2. Methods

### (a) Protein purification and crystallization

Crystals of cloned wild-type T4 glutaredoxin were prepared essentially according to the method of Sjöberg & Söderberg (1976) in the presence of Cd<sup>2+</sup> and with ethanol as the precipitant. These crystals had dimensions of 1·0 mm × 0·25 mm × 0·15 mm. They belong to space-group P2<sub>1</sub> with cell dimensions of  $a = 54\cdot1$  Å,  $b = 45\cdot9$  Å,  $c = 40\cdot8$  Å and  $\beta = 99\cdot4^\circ$  with 2 molecules in the asymmetric unit.

Mutant T4 glutaredoxin was prepared according to the procedure of Joelson *et al.* (1990). Crystals of the mutant T4 glutaredoxin were grown by the hanging drop vapor diffusion method in Costar dishes at 20°C. Droplets (10 µl), which initially contained 15 mg protein/ml, 5% (w/v) polyethyleneglycol 4000 and 25 mM 2-(N-morpholino)ethanesulfonic acid (Mes) pH 6·0 were equilibrated against reservoirs containing 1 ml of 10% (w/v) polyethyleneglycol 4000, 50 mM Mes, pH 6·0. Cd<sup>2+</sup> was not present. The largest crystals were 0·7 mm × 0·8 mm × 0·8 mm. The space group is P2<sub>1</sub>2<sub>1</sub>2<sub>1</sub> and the unit cell dimensions are  $a = 30\cdot2$  Å,  $b = 47\cdot8$  Å and  $c = 61\cdot3$  Å, which gives a unit cell volume of 88,500 Å<sup>3</sup>, 1 molecule per asymmetric unit and a packing density parameter  $V_m$  (Matthews, 1968) of 2·2 Å<sup>3</sup>/dalton.

### (b) Native data sets

A 2·0 Å resolution data set was collected on crystals prepared as described by Söderberg *et al.* (1978) on a single-counter Stoe 4-circle diffractometer. Seven crystals were used to measure a total of 35,300 reflections, which were scaled together using the PROTEIN program (Steigemann, München) giving a data set with 13,500 unique reflections (98% of all possible reflections to 2·0 Å, 90% of all reflections between 2·03 and 2·00 Å). The overall  $R_{\text{merge}}$  for this intersealing was 8·1%, based on intensities ( $R_{\text{merge}} = (\sum I - \langle I \rangle)/\sum \langle I \rangle$ ). This value mainly reflects scaling of many datasets in the resolution range 2·8 to 2·0 Å, where a large part of the reflections are weak. The value of  $R_{\text{merge}}$  for two datasets to 2·8 Å resolution was 3%.

An additional data set was collected on crystals of recombinant T4 glutaredoxin using a Xentronics (Nicolet) multiwire area detector mounted on a Rigaku rotating

anode and evaluated using the Buddha program (Blum *et al.*, 1987). The data set was collected to 2·1 Å resolution, but the reflections were weak beyond 2·3 Å. The reflections were scaled by Rotavata/Agrovata (CCP4, Daresbury, England).

### (c) Data sets of mutant glutaredoxin

A data set to 1·8 Å resolution was collected on 1 crystal on the Xentronics multiwire area detector, evaluated using the Buddha program (Blum *et al.*, 1987) and scaled by Rotavata/Agrovata (CCP4, Daresbury, England). A total of 7223 unique reflections were measured and the  $R_{\text{sym}}$  was 3·4% ( $R_{\text{sym}} = \sum (I - \langle I \rangle)/\sum \langle I \rangle$  for symmetry-related reflections for 1 crystal).

Subsequently, 2 data sets were collected on beam line X31 at the synchrotron at EMBL in Hamburg using the Fuji image plate as detector and the scanner constructed by J. Hendrix. The first data set (with  $\lambda = 0\cdot7$  Å) gave maximum resolution 1·3 Å. In addition, a low resolution data set was recorded to 2·0 Å resolution. Data were processed using the modified MOSCO program package (Nyborg & Wonacott, 1977). The 2 data sets were merged with reflections to 1·45 Å resolution. Reflections to 1·3 Å resolution were too weak to be included. A total of 15,227 unique reflections were measured with a value of  $R_{\text{merge}}$  of 7·3%. The dataset contains 92% of all possible reflections to 1·45 Å (91% of all reflections between 1·52 and 1·45 Å).

Finally, data from the rotating anode and the synchrotron were combined and scaled by the CCP4 programs Agrovata and Rotavata. The  $R_{\text{merge}}$  for all reflections was 5·2%.

### (d) Crystallographic refinement of the wild-type protein

The isomorphous map was of good quality in pleated sheet strands and helices, while connecting loops were less well defined. The map was poor for residues 8 to 13, 43 to 48 and 57 to 64 for both subunits. The strong electron density for the cadmium atoms as well as disturbances around heavy-atom positions distorted corresponding regions. The 1st model of the protein was built using the original version of BILDER (Diamond, 1982) and remodeled before the refinement using FRODO (Jones, 1978).

The co-ordinates from the original model were first refined using the constraint-restraint refinement program CORELS (Sussmann *et al.*, 1977). The position of each amino acid residue was refined as a group with internal torsion angles as additional parameters. The bond between each residue was restrained. Further refinement was performed using EREF (Jack & Levitt, 1978), PROLSQ (Hendrickson & Konnert, 1980) and finally Xplor (Brünger *et al.*, 1987).

After every full cycle of refinement, maps with amplitudes ( $|F_o| - |F_c|$ ) and ( $|F_o| + |F_c|$ ) and with phases calculated from the current model were computed. The model was refitted into these maps and regularized to standard geometry using FRODO (Jones, 1978, 1982, 1985). Ambiguous regions were reinterpreted using maps without contribution of corresponding atoms to the phase and structure factor calculation.

Water molecules were not introduced until the refinement had reached an  $R$ -factor of 0·30 at 2·0 Å. At this point, 14 water molecules were localized from an ( $|F_o| - |F_c|$ ) map and thereafter water molecules were added each time the model was analyzed with computer graphics. An overall temperature factor was used until late in the refinement.

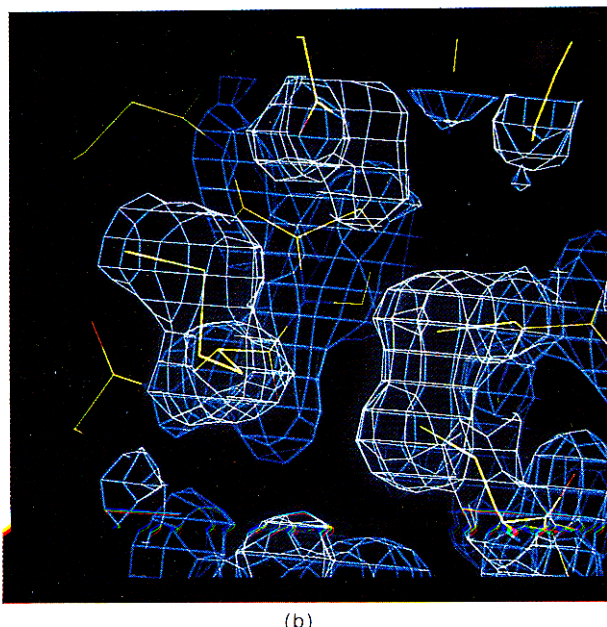
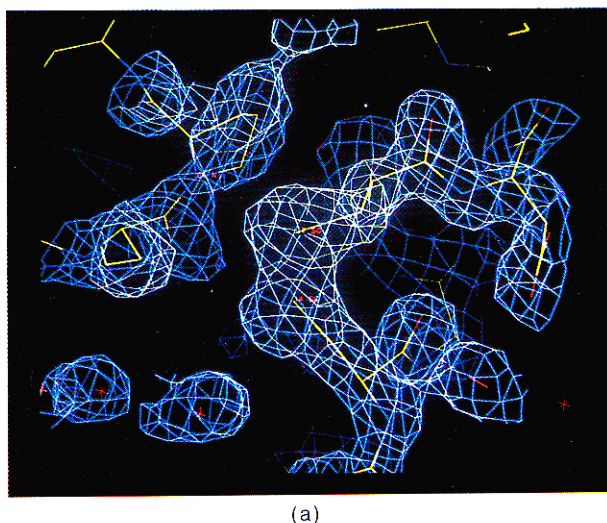


**Figure 2.** Electron density maps of wild-type T4 glutaredoxin. The active site cysteine residue and its environment in wild-type (a) molecule A and (b) molecule B in the final  $2|F_o| - |F_c|$  map contoured at  $1\sigma$ .

(e) *Molecular replacement of the mutant T4 glutaredoxin*

The refined wild-type molecule of T4 glutaredoxin was positioned in the crystals of the mutant protein by molecular replacement methods. A rotation function search was performed using the program Polarrfn, written by Wolfgang Kabsch, Heidelberg, Germany and incorporated in the CCP4 program package (Daresbury Laboratory, England). A radius of 15 Å was used in the resolution range 10 to 2.6 Å. Only 1 prominent peak was found, which was twice as high as the 2nd peak. The position of the rotated molecule was investigated using a translation function (Tfsgen) (Tickle, 1985) with a 0.6 Å grid using a radius of 20 Å in the resolution range 20 to 2.5 Å. Only 1 prominent peak (and its symmetry-related peaks) was found. The second-highest peak significantly different from the 1st was lower than half of the 1st peak.

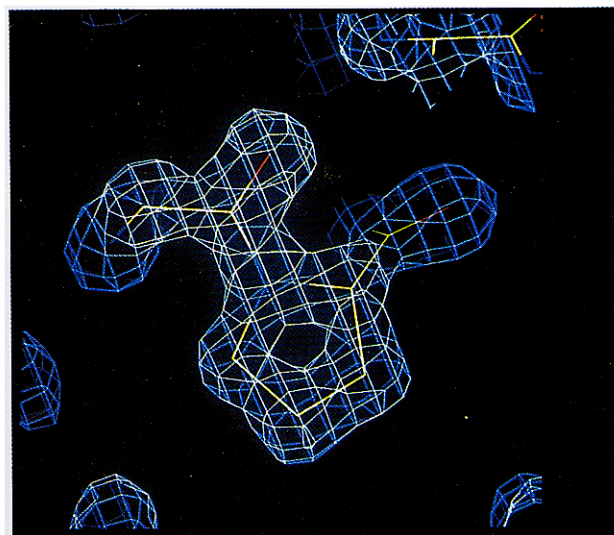


**Figure 3.** Electron density maps of mutant glutaredoxin in the vicinity of mutated residues. Residues 15 and 16 have been mutated from Val-Tyr to Gly-Pro. (Final  $2|F_o| - |F_c|$  map contoured at  $1.5\sigma$ .)

(f) *Refinement of the glutaredoxin mutant protein*

The rotated and translated glutaredoxin molecule gave an *R*-value of 42% in the resolution range 8.0 to 4.0 Å (47.3% in the resolution range 8.5 to 1.8 Å). The residues at the active site were changed to Gly-Pro before the simulated annealing of the structure using Xplor (Brünger *et al.*, 1987). The *R*-value was lowered to 29.9% (7.0 to 1.8 Å) after the 1st run. Temperature-factor refinement, inclusion of water molecules and positional refinement of Jack-Levitt type further decreased the value of *R*-factor.

Co-ordinates of the 2 wild-type molecules (1AAZ) and the mutant glutaredoxin (1ABA) as well as structure factors for both crystal forms have been deposited in the Brookhaven Protein Data Bank.

### 3. Results and Discussion

The wild-type and mutant T4 glutaredoxins have been refined to *R*-values of 0.209 and 0.175, respectively. In the final models of wild-type and mutant glutaredoxin, the deviation from ideal bond distances are 0.011 Å and 0.012 Å, the deviation for bond angles 2.87° and 2.53° and for dihedral angles 25.3° and 24.5°.

In the final maps, most of the residues are well defined (Figs 2, 3 and 4) including the carbonyl oxygen atoms of the main chain, side-chain atoms and the first layer of water molecules. One exception is the loop 57–62 in both wild-type molecules, which is still disordered after the refinement and there is only weak density for these residues. This loop is well ordered in the mutant glutaredoxin structure due to inter-molecular interactions in the crystal.

The Ramachandran plots are very similar for the two wild-type molecules and for the mutant protein (Fig. 5) and the r.m.s. deviation of the  $\phi$  and  $\psi$  angles between different molecules is 7°. Most of the

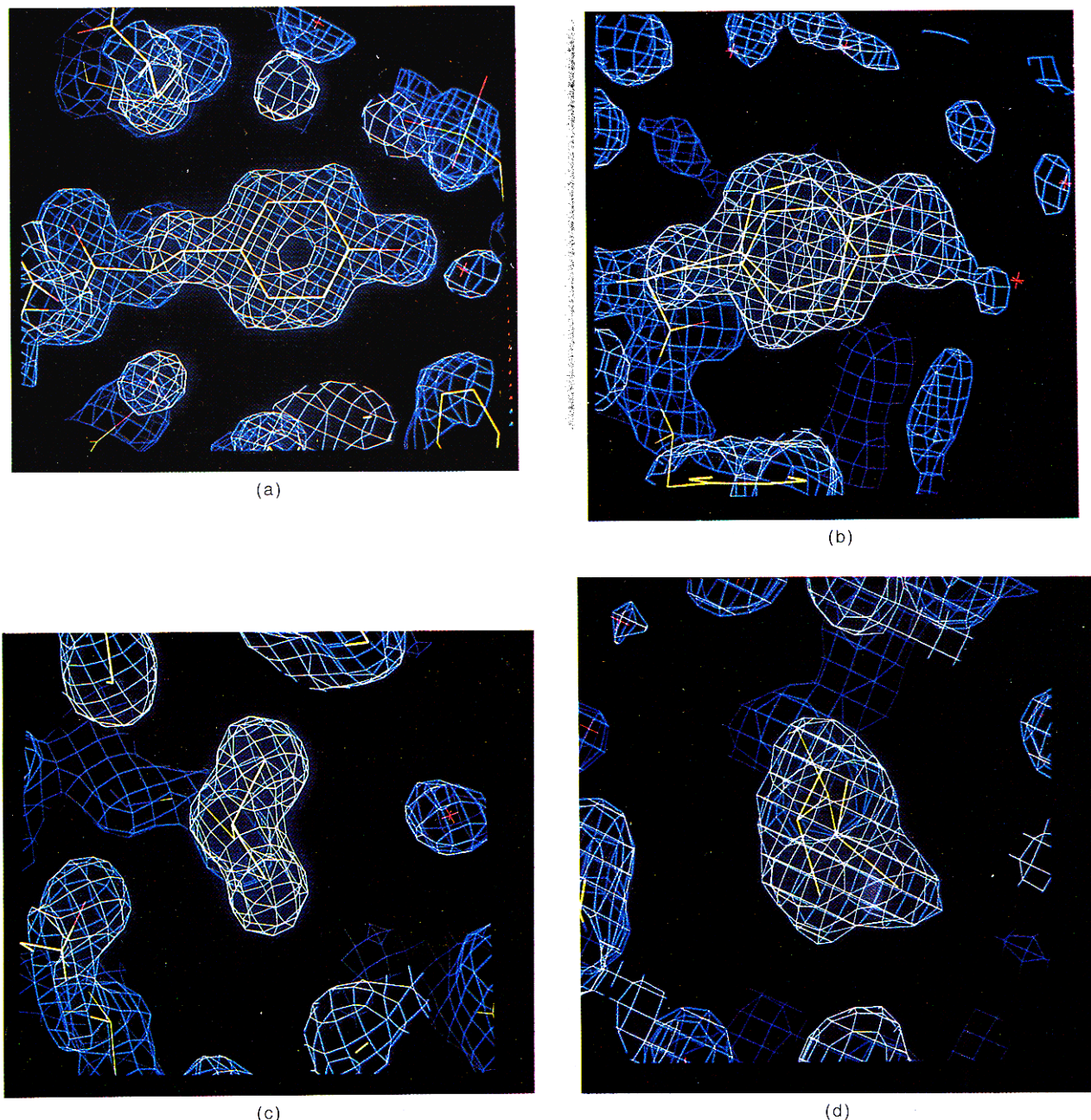


**Figure 4.** Electron density maps of mutant glutaredoxin. The electron density  $2|F_o| - |F_c|$  contoured at  $1\sigma$  for (a) a normal tyrosine (Tyr7) and (b) Tyr85 for which the electron density map indicates 2 conformations, (c) for a normal leucine (Leu85) and (d) the density for Leu55 indicating 2 conformations. Both conformations have been treated as half occupied and no attempts have been made to refine the occupancies of the individual conformations.

residues which have positive  $\phi$  angles are glycines (at position 41, 56, 62, 73 and 77). The only non-glycine is Lys28 at the end of the  $\alpha 1$  helix. This type of helix end is common (Schellman, 1980; Baker & Hubbard, 1984) and usually contains a Gly in the corresponding position.

#### (a) Overall structure

The general description of the T4 glutaredoxin structure given here is relevant for all three molecules in this investigation. A comparison between the three molecules is made below.

From one side (Fig. 6(d)), the shape of the molecule is rectangular with the approximate dimensions 20 Å and 25 Å for the sides of the rectangle, and about 40 Å in the longest dimension. The main chain of the T4-glutaredoxin molecule can be described as a funnel with a thick spout with part of the edge of the funnel missing (Fig. 6(c)). The end of the spout is at the two ends of the polypeptide chain, while the redox-active disulfide is inside the funnel.

T4 glutaredoxin belongs to the  $\alpha/\beta$  class of proteins (Levitt & Chothia, 1976) which have a central pleated sheet surrounded by helices. The central

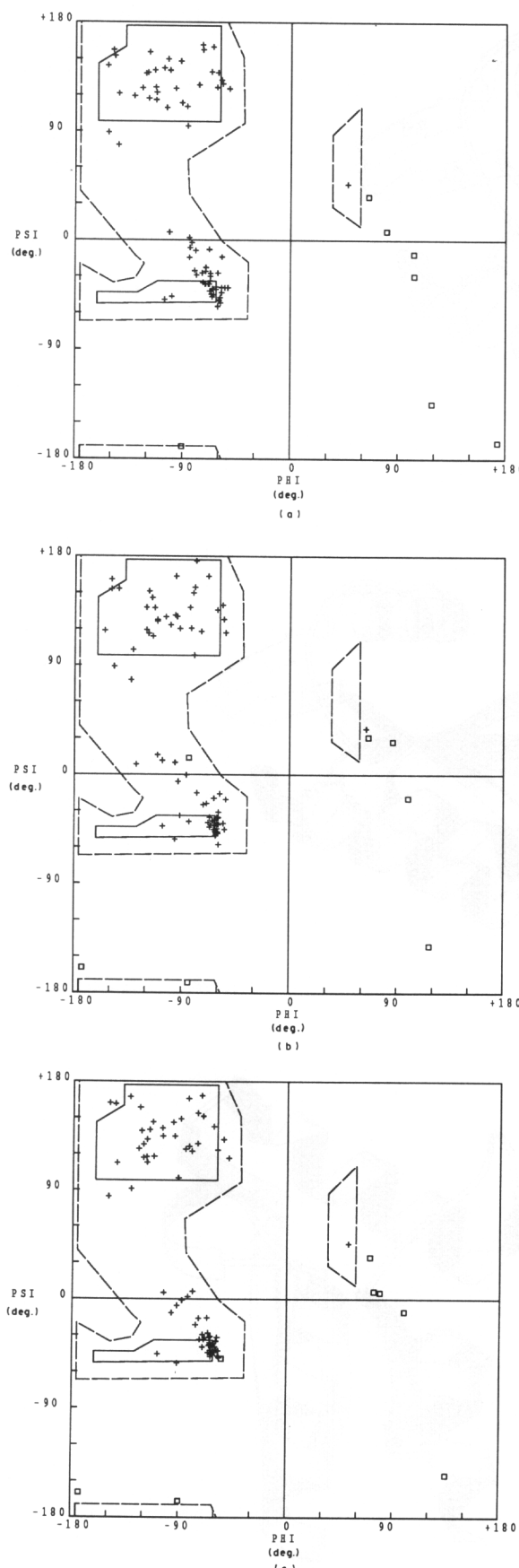


**Figure 5.** Ramachandran plots. (a) Wild-type molecule A, (b) wild-type molecule B, (c) the mutant T4 glutaredoxin. Glycine residues are plotted as boxes to distinguish them from other residues.

**Table 1**  
Secondary structure elements in T4 glutaredoxin

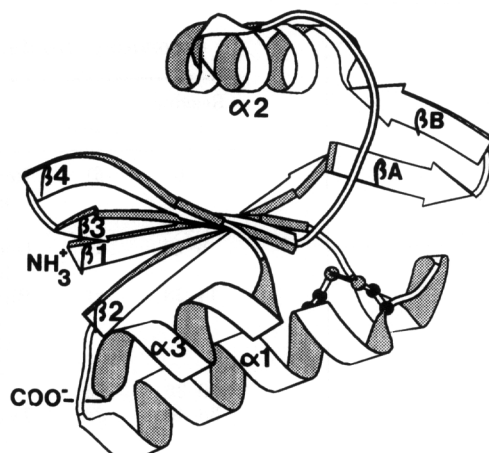
| Residue no. | Name       | Comments   |
|-------------|------------|--|
| 2–6         | $\beta 1$  | Residue 1 has no hydrogen bond to the main chain but has extended strand conformation                          |
| 8–12        | $\alpha T$ | One turn of $\alpha$ -helix with also one 3 <sub>10</sub> hydrogen bond (8O–N11, N12)                          |
| 14–28       | $\alpha 1$ | Bifurcated hydrogen bonds at the carboxyl end between 24O–N28, N29. One 1–4 bond at the carboxyl end (25O–N28) |
| 30–36       | $\beta 2$  |  |
| 36–40       | $\beta A$  | Two hydrogen bonds only between $\beta A$ and $\beta B$ : 36O–N44 and 39O–N42                                  |
| 41–44       | $\beta B$  |  |
| 44–55       | $\alpha 2$ | Bifurcated hydrogen bonds at the amino end between 44O–N47, N48 and at the carboxyl end between 52O–N56, N57   |
| 66–71       | $\beta 3$  | Residue 66 has no pleated sheet hydrogen bond  |
| 72–77       | $\beta 4$  | $\beta$ Bulge at Gly73   |
| 78–87       | $\alpha 3$ | Distorted at the end, 82O–N86 3·4 to 3·5 Å, no 83O–N87 hydrogen bond but a 84O–N87 bond at the end             |

pleated sheet consists of four strands with two  $\alpha$ -helices on one side roughly parallel to the strands of the pleated sheet and with one  $\alpha$ -helix on the other side roughly perpendicular to the strands of the pleated sheet. The molecule consists of two distinct folding units which are seen in Figure 6. The first unit is essentially a  $\beta\alpha\beta$  unit which is connected to the second, a  $\beta\beta\alpha$  unit with an anti-parallel hairpin, an  $\alpha$ -helix plus loops on one side of the pleated sheet.

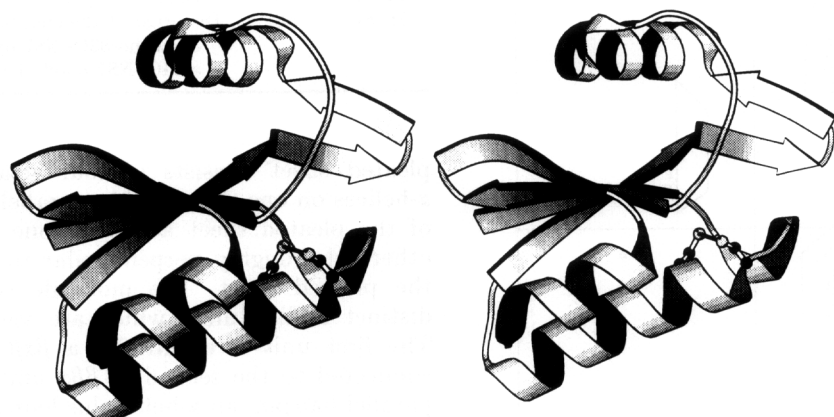
The strand order in the  $\beta$ -sheet is  $\beta 2$ ,  $\beta 1$ ,  $\beta 3$  and  $\beta 4$  with the third strand of the sheet antiparallel to the others. The hydrogen-bonding pattern is anti-parallel between three of the strands and parallel only between the two first strands (Fig. 7). The topology of the pleated sheet –1, +2, +1 (Richardson, 1977) is similar to that of thioredoxin from *E. coli*, but *E. coli* thioredoxin contains one additional  $\beta$ -strand and one helix at the amino terminus of the molecule and its topology is +2, –1, +2, +1. For the comparison, it was convenient in the first report to use the same nomenclature for the two proteins (Söderberg *et al.*, 1978). We will not keep this nomenclature in this paper and the T4 glutaredoxin will now be described starting with  $\beta 1$  (Fig. 6(a)). The fold of the glutaredoxin molecule is the same as domain I in glutathione transferase (Reinemer *et al.*, 1991).

All hydrogen bonds between main-chain atoms are drawn schematically in Figure 7 and more detailed stereo-drawings in Figure 8. The assignment of secondary structural elements are summarized in Table 1.

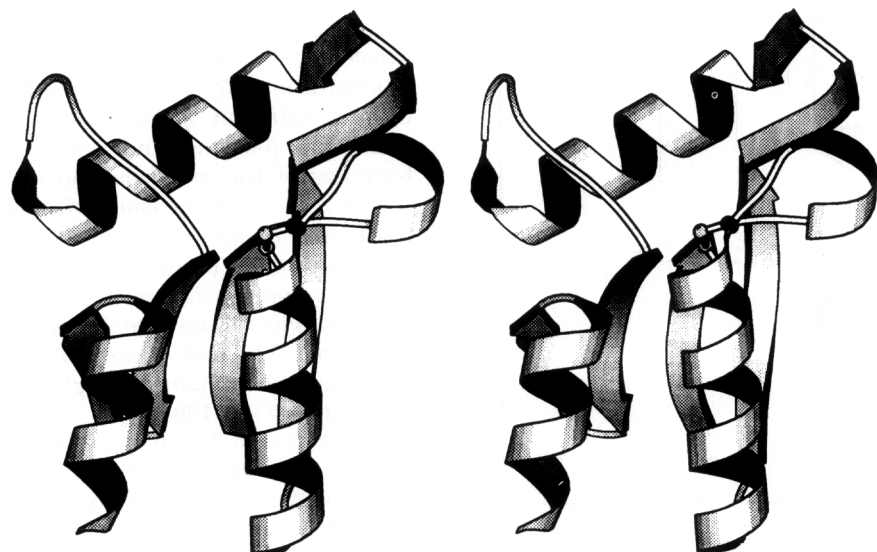
In T4 glutaredoxin, 21 of the 87 residues constitute the five bends in the structure (Table 2). There is also a reverse turn hydrogen bond between residues 84 and 87 at the end of  $\alpha 3$ . Residues 8 to 12



( a )



( b )



( c )

**Fig. 6.**

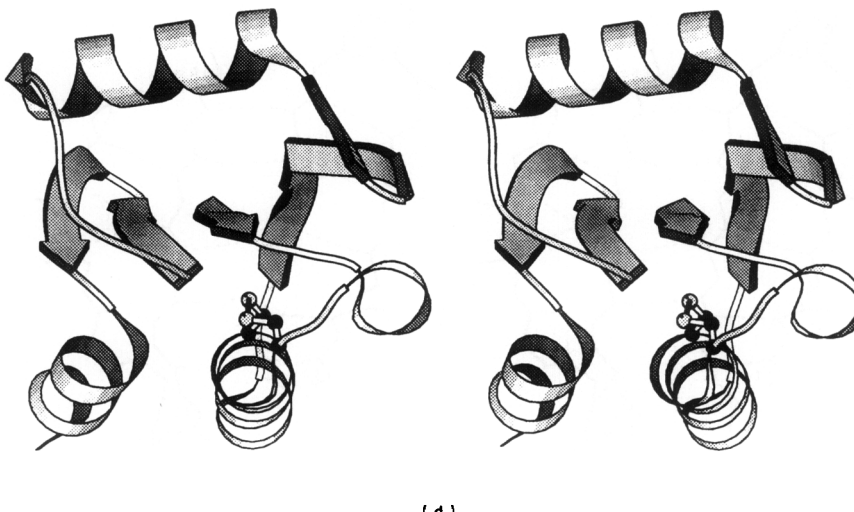


**Figure 6.** Ribbon drawings of the main chain of T4 glutaredoxin. The drawings (a) to (d) have been made using the Molscript program by Per Kraulis (1991). (a) The main chain of T4 glutaredoxin with the names of the secondary structure elements. (b) The main chain of the T4 glutaredoxin molecule viewed along the pleated sheet strands with  $\alpha_1$  and  $\alpha_3$  under and along the sheet and  $\alpha_2$  over and perpendicular to the sheet. (c) The main chain of the T4 glutaredoxin molecule viewed perpendicular to the pleated sheet with the strands of the 1st folding unit to the left and the strands of the 2nd folding unit to the right. The molecule is opened up at the top as a funnel with the active site down in the funnel.  $\alpha_2$  is on top and  $\alpha_1$  to the right and  $\alpha_3$  to the left. (d) The main chain of the T4 glutaredoxin molecule viewed along the pleated sheet with  $\alpha_2$  on top and  $\alpha_3$  and  $\alpha_1$  at the bottom.

form a turn of helix ( $\alpha_T$ ) with a hydrogen bond between the main-chain oxygen atom of residue 8 and main-chain nitrogen atoms of residues 11 and 12 in a mixed  $3_{10}$  and  $\alpha$ -helix turn.

There is a long stretch of extended chain from residues 29 to 40 with residues 30 to 36 in the regular hydrogen-bonded part of the main pleated sheet. Residue 36 makes a kink in the chain which turns away from the pleated sheet in the same region as  $\alpha_T$ . Residues 36 to 44 form a short anti-parallel hairpin loop ( $\beta_A-\beta_B$ ) with a hydrogen bond between residues 36 and 44 and a  $\beta$ -bend of type II at its tip formed by residues 39 to 42 with Gly in the third position, as is frequently found for this type of bend. The hydrogen bonding in this antiparallel hairpin is disrupted by a bulge and its first half, the strand 36–40, is one residue longer than its second half, residues 41–44. Pro38 makes the kink in this hairpin (Fig. 8(b)) and has helix main-chain torsion angles. Due to this, Glu39N is too far from the carbonyl group of residue 42 to form a hydrogen bond. Residues 60 to 63 form a reverse turn, which is the only ordered hydrogen-bonded structure in the loop 57–65.

Pro66 is in the *cis*-configuration. The bend between  $\beta_3$  and  $\beta_4$  is somewhat wider than a regular  $\beta$ -bend due to a  $\beta$ -bulge of classical type (Richardson, 1981), where residue 73 is a Gly and residue 70 makes hydrogen bonds to Gly73 N and Ser74 O. The strand  $\beta_4$  with residues 72 to 77 is unusual since the torsion angles are in the strand region only for residues 74 and 75. The beginning is deformed by the bend and the  $\beta$ -bulge, but also, residue 76 breaks the regular strand pattern and the main-chain torsional angles for this residue are in the helix region which bends the strand (Fig. 8(a)).

The main-chain oxygen atom of residue 68 forms hydrogen bonds to nitrogen atoms of residues 76 and 77.

#### (b) Main-chain-side-chain hydrogen bonds

Polar main-chain atoms are commonly involved in internal hydrogen bonds within secondary structure elements; however, at the helix termini and for

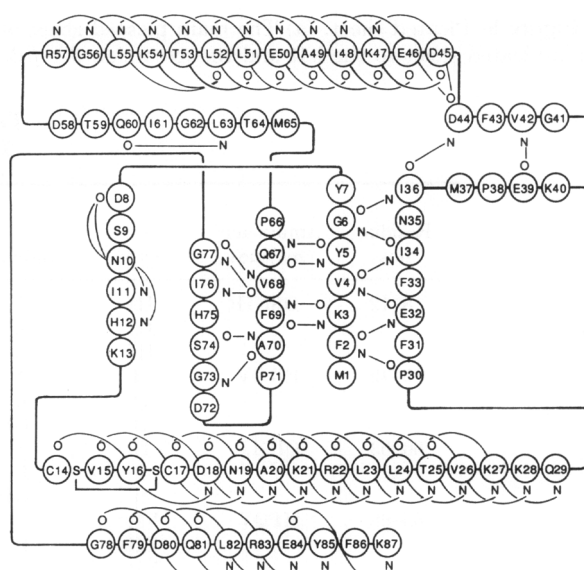


**Figure 7.** Hydrogen bonding scheme. Schematic drawing of the main-chain hydrogen bonding in T4 glutaredoxin. According to normal conventions, we have assigned a hydrogen bond when donor and acceptor atoms are closer than 3.3 Å.

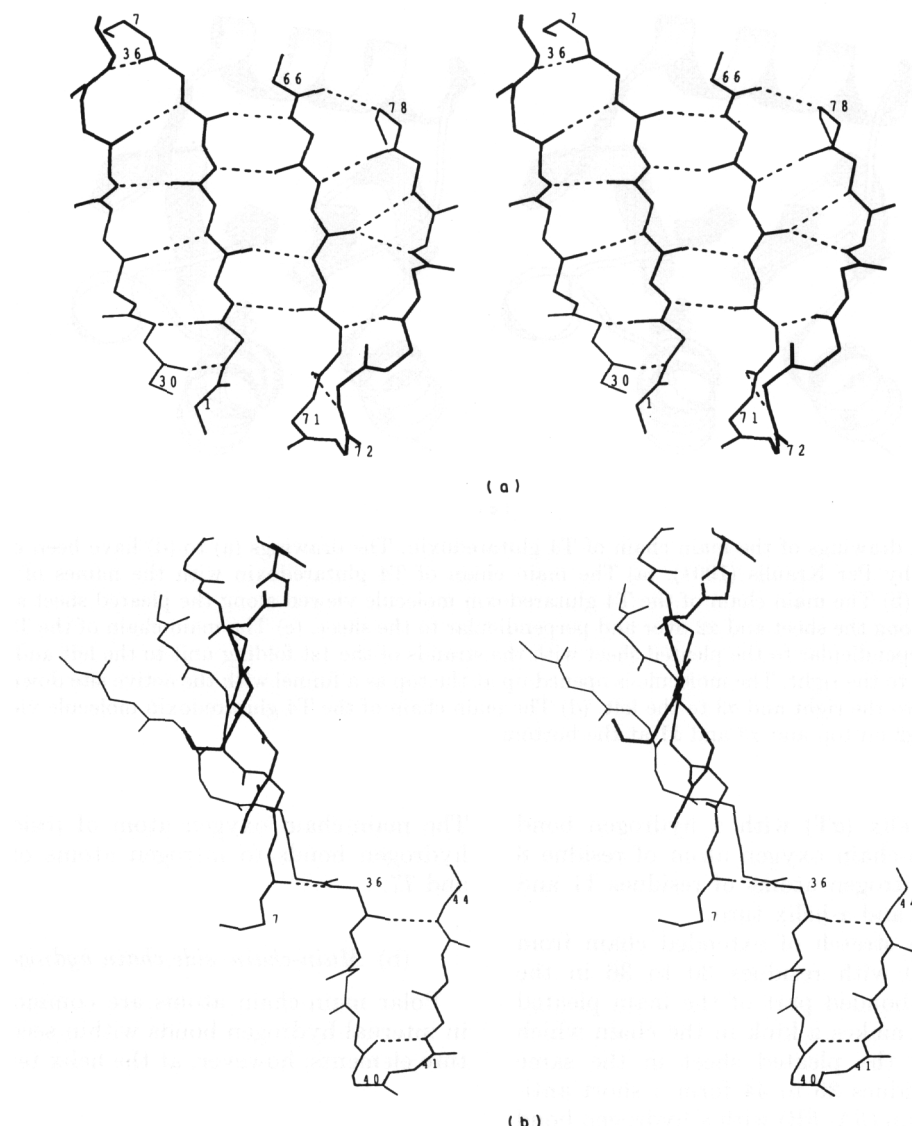


**Figure 8.** Pleated sheet. (a) The main pleated sheet of T4 glutaredoxin. (b)  $\beta$ -Structure in T4 glutaredoxin with the main pleated sheet to the left and the excursion  $\beta$ A- $\beta$ B to the right.

**Table 2**  
*Turns*

| Residue nos | Amino acid residues | Type | Subunit† | Ramachandran angles (deg.) |          |          |          |            | Comments |
|-------------|---------------------|------|----------|----------------------------|----------|----------|----------|------------|----------|
|             |                     |      |          | $\Phi$ 2                   | $\Psi$ 2 | $\Phi$ 3 | $\Psi$ 3 |            |          |
| 8–12        | DSNIH               | III  | A        | −57                        | −14      | −71      | −23      | $\alpha$ T |          |
|             |                     | III  | B        | −58                        | −15      | −77      | −15      |            |          |
|             |                     | III  | GP       | −67                        | −16      | −74      | −15      |            |          |
| 39–42       | EKGV                | II   | A        | −51                        | 125      | 80       | 7        | Turn 1     |          |
|             |                     | II   | B        | −54                        | 117      | 65       | 31       |            |          |
|             |                     | II   | GP       | −49                        | 117      | 79       | 5        |            |          |
| 60–63       | QIGL                | II   | A        | −62                        | 126      | 103      | −29      | Turn 2     |          |
|             |                     | I    | B        | −84                        | −39      | −84      | 14       |            |          |
|             |                     | II   | GP       | −59                        | 123      | 73       | 6        |            |          |
| 65–68       | MPQV                | VIb  | A        | −74                        | 162      | −124     | 126      | Turn 3     |          |
|             |                     | VIb  | B        | −79                        | 176      | −120     | 119      |            |          |
|             |                     | VIb  | GP       | −83                        | 166      | −125     | 124      |            |          |
| 70–73       | APDG                | I    | A        | −60                        | −27      | −84      | −6       | Turn 4     |          |
|             |                     | I    | B        | −57                        | −20      | −106     | 12       |            |          |
|             |                     | I    | GP       | −59                        | −31      | −83      | 2        |            |          |

† Subunits A and B refer to the 2 subunits in the wild-type glutaredoxin, while GP refers to the mutant glutaredoxin.

**Table 3**  
*Hydrogen bonds from side-chains to main-chain atoms in T4 glutaredoxin*

| Main-chain atom | Residue and atom | Comment  |
|-----------------|------------------|--|
| N7              | Cys17 SG         | Active site S-NH hydrogen bond                                 |
| N8              | Asn35 OD1        | At the amino end of $\alpha$ T (only in the mutant)            |
| N10             | Asp8 OD2         | At the amino end of $\alpha$ T                                 |
| N14             | Ser9 OG          | Connects $\alpha$ T with $\alpha$ 1, amino end of $\alpha$ 1   |
| N17             | Cys14 SG         | Active site S-NH hydrogen bond                                 |
| O21             | Thr25 OG1        | In the middle of the helix, $\alpha$ 1                         |
| N37             | Asn35 OD1        | Residue 35 is on the exposed side of $\beta$ 2                 |
| O37             | Asn35 ND2        | (Only in the mutant glutaredoxin)                              |
| N47             | Asp44 OD2        | At the amino end of $\alpha$ 2                                 |
| O49             | Thr53 OG1        | In the middle of the helix, $\alpha$ 2 (not in the molecule B) |
| O59             | Arg57 NH1        | At the surface (only in the mutant glutaredoxin)               |
| O61             | Arg57 NH1        | At the surface (only in the mutant glutaredoxin)               |
| O64             | Gln67 NE2        | Hydrogen bond in the type VIa turn                             |
| N74             | Asp72 OD1        | In a reverse turn (only in the mutant glutaredoxin)            |
| N78             | Gln81 OE1        | At the amino end of $\alpha$ 3 (not in molecule B)             |

strands at either end of a sheet, some polar main-chain atoms are exposed to solvent. No main-chain-main-chain hydrogen bonds are present for 16 residues: Met1, Tyr7, Lys13, Phe31, Phe33, Asn35, Met37, Pro38, Phe43, Asp58, Thr59, Thr64, Met65, Pro66, Pro71 and Asp72. In some of these cases, well-ordered water molecules can be found hydrogen

bonded, while in other cases, side-chains form hydrogen bonds to these main-chain atoms (Table 3). All helices have at least one side-chain hydrogen bond to an amino end nitrogen atom. For  $\alpha$ T and  $\alpha$ 2, the hydrogen bond is formed by an aspartic acid. Ser9 connects  $\alpha$ T with  $\alpha$ 1, not only with the side-chain hydrogen bond to the nitrogen atom of residue 14, but also with a hydrogen bond to the side-chain of Asp18 in the first turn of  $\alpha$ 1. The hydrogen bonds to the disulfide bridge are discussed below.

The *cis*-Pro bend (type VIb) has no 1-4 hydrogen bond, but the bend in T4 glutaredoxin is stabilized by a hydrogen bond from the side-chain of Gln67 to N64. This is very similar to the stabilization of the corresponding bond in *E. coli* thioredoxin, where Thr77 makes a hydrogen bond to the nitrogen atom of residue 74.

### (c) Packing between secondary structure elements

In most  $\alpha/\beta$  structures, the pleated sheet is covered on both sides by helices, which are packed against the sheet by hydrophobic interactions (Chothia *et al.*, 1977). In T4 glutaredoxin, one side of the four-stranded sheet is fully covered by the two helices,  $\alpha$ 1 and  $\alpha$ 3, which are approximately parallel to the corresponding strands. On this side, the pleated sheet packs against helix  $\alpha$ 1 with residues from strand  $\beta$ 1,  $\beta$ 2 and  $\beta$ 3 (Fig. 9). The interior of this part forms a hydrophobic core. Contacts between the pleated sheet and helix  $\alpha$ 3 involve side-chains from all four strands.

However, on the other side of the sheet there is only one helix,  $\alpha$ 2, which lies obliquely across the

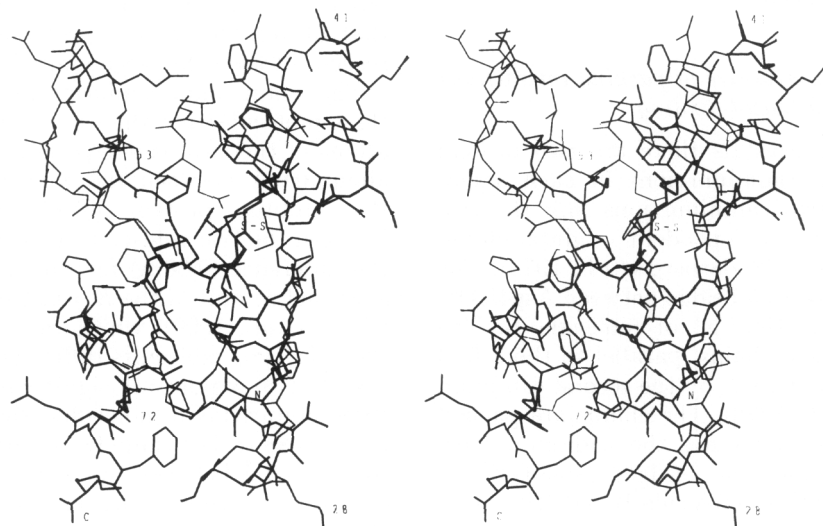


**Figure 9.** The T4 glutaredoxin wild-type molecule A with all side-chains. There is one hydrophobic core on the front side with Phe2, Val4, (Cys14), Cys17, Ala20, Leu23, Leu24, Phe31, Phe33, Pro66, Val68, Ile76, Phe79, Leu82, Phe86, Tyr85 and another hydrophobic core on the back side with Tyr5, Tyr7, Ile34, Met37, Phe43, Ile48, Leu51, Leu55, Leu63, Met65 and Phe69. Side-chains of residues Phe2, Val4, Phe31, Phe33 and Pro66 from the pleated sheet, pack against side-chains of residues Tyr16, Cys17, Ala20, Lys21 and Leu24 of  $\alpha$ 1. Residues Phe2, Val4, Gln29, Thr68, Pro71 and Ile76 of the pleated sheet pack against side-chains of Leu82, Tyr85 and Phe86 of the  $\alpha$ 3. Contacts between these 2 helices involve residues Ala20, Leu23 and Leu24 of  $\alpha$ 1 and Phe79, Leu82 and Arg83 of  $\alpha$ 3. Side-chains Tyr5, Ile34, Ile36, Glu67, Phe69 and His75 at the edge of the pleated sheet make contacts with side-chains of Lys47, Ile48, Glu50, Leu51, Lys54 and Leu55 of  $\alpha$ 2.

sheet and covers only part of it.  $\alpha 2$  does not pack against the main surface of the sheet, but covers only one edge of the sheet. The angle is approximately  $65^\circ$  between the helical axis and the direction of the strands. Most of this side of the pleated sheet is uncovered by other structural elements at the surface. Residues such as Met1, Lys3, Pro30 and Glu32 are exposed and point into the solution on this side. In a fully covered  $\alpha/\beta$  protein, these residues would be buried and thus mainly non-polar.

#### (d) Surface residues

All of the charged and most of the polar side-chains are located at the surface of the molecule in contact with the surrounding solvent (Fig. 9). There is a surplus of positive charges at the carboxyl ends of the helices and a surplus of negative charges around the amino ends of helices. Some charged residues form hydrogen bonds to other side-chains. In only three cases are there hydrogen bonds between side-chains of sequentially more distant residues: Glu50 and Lys54 from  $\alpha 2$  makes hydrogen bonds to the tyrosine hydroxyl group of residue 5 of  $\beta 1$ , Asp18 in  $\alpha 1$  makes a hydrogen bond to Ser9 from  $\alpha T$  and Gln67 in  $\beta 3$  forms a hydrogen bond to His75 in  $\beta 4$ . Asn35 also contributes to the binding of  $\alpha T$  to the main body of the structure. This residue forms hydrogen bonds to three main-chain atoms in the mutant glutaredoxin structure.

A region comprising residues 7, 14 to 16, 37, 41 to 43 and 59 to 66 defines a surface region including the active site which was suggested to interact with thioredoxin reductase and ribonucleotide reductase (Eklund *et al.*, 1984). This part of the surface is devoid of charged residues.

#### (e) The effect on the structure of packing interactions and metal binding

In the wild-type crystals there are two protein molecules and two cadmium ions in each asymmetric unit. The two cadmium ions link the two crystallographically independent glutaredoxin molecules into dimers (Söderberg *et al.*, 1978). The first cadmium ion forms a bridge between Asp45 O<sup>δ1</sup> of molecule A and His75 N<sup>ε</sup> of molecule B. The dimers are linked into chains, parallel to the 2-fold crystallographic screw-axis, by the second cadmium ion (Söderberg *et al.*, 1978). The chains are packed into layers without involving the cadmium ions. The second cadmium ion bridges Glu39 O<sup>ε1</sup> of molecule A, Asp72 O<sup>δ1</sup> of molecule B and His12 of a symmetry-related molecule B.

Both cadmium ions have octahedral coordination geometry (Fig. 10). The first cadmium ion is bound by only two protein ligands, His75 and Asp45, but the aspartic acid is a bidentate ligand with one oxygen atom at a longer distance to the cadmium ion than the second carboxyl oxygen atom. The remaining ligands are water molecules. The second cadmium ion is bound by an Asp and a

Glu in a square planar arrangement with water molecules at the other vertices. His12 and a water molecule lie above and below the plane, completing the bipyramid.

The association between glutaredoxin molecules in the wild-type crystals is quite heterologous, due to the binding to the two cadmium ions. This heterologous packing has the consequence that practically all sides of the molecule are involved in different associations in the two molecules. As much as half of all residues are involved in packing interactions (Table 4). There are many van der Waals' contacts between molecules and 15 residues are involved in hydrogen bonds between neighboring molecules.

It appears that  $\alpha 3$  is important for the packing of molecules in the orthorhombic crystals of the mutant glutaredoxin. The carboxyl end of the molecule (at the end of  $\alpha 3$ ) forms two hydrogen bonds to the main-chain amino group of the residues 79 and 80 (at the beginning of  $\alpha 3$ ) in another molecule (Fig. 10(c)).

#### (f) Comparison of the three molecules

The three molecules in this investigation were compared using the program O (Jones *et al.*, 1990). Different superpositions were investigated and the best overlap of the secondary structure elements was obtained by superimposing the C<sup>α</sup> atoms of residues 1 to 35, 44 to 56 and 65 to 87. These residues have been used to superimpose the three molecules for the discussion of the differences below. In the comparison with the mutant glutaredoxin, a superposition of residues 2 to 37, 44 to 55, 66 to 71 and 73 to 79 gives a slightly better similarity but is based on fewer residues. The difference is mainly that  $\alpha 3$  (residues 80 to 87) is translated slightly with respect of the other secondary structure elements.

The main-chain conformation is similar in the three molecules and the r.m.s. difference between C<sup>α</sup> atoms of the two wild-type molecules is 0.52 Å and about 0.9 Å between the wild-type molecules and the mutant protein (Table 5). The difference between the two wild-type molecules is smaller than the difference (0.66 Å) for the two molecules in the asymmetric unit of the *E. coli* thioredoxin structure (Katti *et al.*, 1990), while the mutant protein and the wild-type molecules differ more.

Only two regions are significantly different in the three glutaredoxin molecules, the antiparallel loop, residues 38 to 44 (where the position of Gly41 differs by 1.5 to 2 Å between the 3 molecules) and the less-ordered part, comprising residues 56 to 65 (Fig. 11). Furthermore, the position of  $\alpha 3$  is slightly different in the three molecules.

The largest difference between the mutant glutaredoxin structure and the wild-type molecules is for the loop of residues 56–64, which has a conformation that differs by as much as 5 Å for main-chain atoms (Fig. 11). While regions of disorder sometimes have specific functions (Bennett & Huber, 1984), there is at the moment no obvious functional

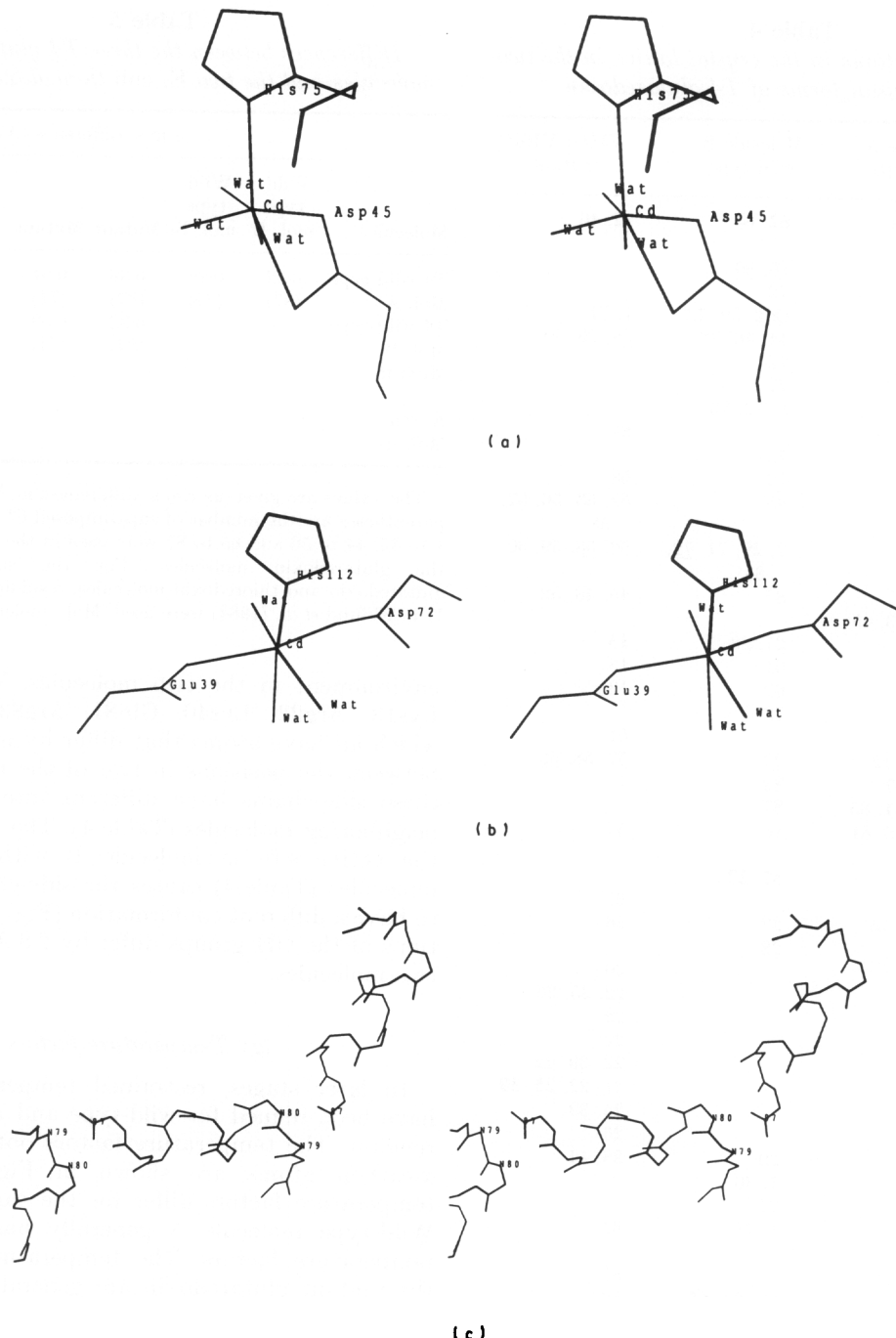


**Figure 10.** Packing interactions in the crystals. Cd co-ordination in wild-type crystals. (a) Cd1 with protein ligands Asp45 which is a bidental ligand and His75 from another molecule. (b) Cd2 with protein ligands His12 (112 in the Fig.), Glu39 and Asp72 from 3 different molecules. The octahedral co-ordination is completed by water molecules in both cases. (c) The interaction of  $\alpha$ 3 in 3 different molecules in crystals of the mutant glutaredoxin. The carboxyl end of the  $\alpha$ 3 in 1 molecule is hydrogen bonded to the main-chain nitrogen atoms in the amino end of  $\alpha$ 3 in the next molecule where the carboxyl end of the  $\alpha$ 3 is hydrogen bonded to the main-chain nitrogen atoms in the amino end of  $\alpha$ 3 in the next molecule and so on.

significance for this flexibility in T4 glutaredoxin. A corresponding region is almost absent from the homologous glutaredoxins (see below), while it is longer in glutathione peroxidase, which has a similar three-dimensional structure (Ladenstein *et al.*, 1979). From molecular dynamics calculations, the large fluctuations of this loop have been suggested to play a functional role in reductase

binding by exposing hydrophobic side-chains (Nilsson, 1991).

Many side-chains have quite different conformations in the three molecules due to the differences in packing (Table 6). This is reflected in the high r.m.s. difference of 2 Å between side-chain atoms. Not surprisingly, some of the long charged or polar side-chains differ significantly due to the different

**Table 4**

*Molecular interactions in the crystal lattice in the two different crystal forms of T4 glutaredoxin*

| Residue | Molecule A<br>wild-type    | Molecule B<br>wild-type                              | V15G; Y16P<br>mutant          |
|---------|----------------------------|--|-------------------------------|
| Met1    | 56, 58                     | <b>62</b> , 64                                       | 12, 40                        |
| Phe2    | 25                         |  |                               |
| Lys3    |                            | 16, <u>80</u>  |                               |
| Tyr7    |                            | 72   |                               |
| His12   |                            | <u>Cd2</u> , 39, 72                                  | 1, 71                         |
| Lys13   |                            | 44, 46, 72   | <u>28</u> , 29, 30            |
| Cys14   |                            | 72   |                               |
| Val15   |                            | 72   |                               |
| Tyr16   |                            | 3, 72, 73  |                               |
| (Pro16) |                            |  | 84                            |
| Cys17   |                            | 72   |                               |
| Lys21   |                            | 72   | 58                            |
| Arg22   | <b>39</b>                  | 85   | 52, 53, 56, <u>57</u> ,<br>58 |
| Thr25   |                            | 2, <b>29</b> , 71, <u>72</u> ,<br>85                 | 52, 58, 59, 60                |
| Val26   | 42                         | 85   | 45, 48, 52                    |
| Lys27   | <b>28</b> , <u>43</u> , 45 |  |                               |
| Lys28   | <b>46</b>                  | 27, 28   | 13                            |
| Gln29   | <b>25</b>                  | 61   | 13                            |
| Pro30   |                            | 62   | 13                            |
| Phe31   |                            | 72   |                               |
| Pro38   |                            |  | 61                            |
| Glu39   | <u>Cd2</u> , 12            | <b>22</b>  | <u>57</u> , 58, <b>59</b>     |
| Lys40   | <u>84</u> , 87             | <b>83</b>  | 1                             |
| Gly41   | 76, <b>81</b> , 85         | <b>87</b>  |                               |
| Val42   | 74, 75, 81,<br>85          | 26   | 57                            |
| Phe43   | 81                         | 87, 27   |                               |
| Asp44   | 13                         |  | 61                            |
| Asp45   | <u>Cd1</u> , 75            | 27   | 26                            |
| Glu46   | 13                         | <b>28</b>  |                               |
| Ile48   |                            |  | 26                            |
| Leu52   |                            |  | 22, 25, 26                    |
| Thr53   |                            |  | 22                            |
| Gly56   | 1                          |  | 22                            |
| Arg57   |                            |  | <b>22</b> , <u>39</u> , 42    |
| Asp58   | 1                          |  | 21, 22, <b>25</b> , <b>39</b> |
| Thr59   |                            |  | 25, <u>39</u>                 |
| Gln60   |                            |  | 25                            |
| Ile61   |                            | 29   | 38, 44                        |
| Gly62   |                            | 1, 30  |                               |
| Leu63   |                            | 71   |                               |
| Thr64   |                            | 1, 71  | 87                            |
| Met65   | <b>71</b>                  |  |                               |
| Pro66   |                            |  | 87                            |
| Pro71   | 25                         | 63, 64, <b>65</b>                                    | 12                            |
| Asp72   | 21, <u>25</u> , 31         | <u>Cd2</u> , 7, 12,<br>13, 14, <b>15</b> ,<br>16, 17 |                               |
| Gly73   |                            | 16   |                               |
| Ser74   |                            | 42   |                               |
| His75   |                            | <u>Cd1</u> , 42, 45                                  |                               |
| Ile76   |                            | 41   |                               |
| Gly78   |                            |  | 87                            |
| Phe79   |                            |  | <b>87</b>                     |
| Asp80   |                            | 3  | 85, 86, <b>87</b>             |
| Gln81   |                            | <u>41</u> , 42, 43                                   |                               |
| Arg83   | <b>40</b>                  |  | <b>85</b>                     |
| Glu84   |                            | 40   | 16                            |
| Tyr85   | 22, 25, 26                 | 41, 42   | 80, <b>83</b>                 |
| Phe86   |                            |  | 80                            |
| Lys87   | <u>41</u> , 43             | 40   | 64, 66                        |
| -COO-   |                            |  | 78, <b>79</b> , <b>80</b>     |

In this Table, all residues in van der Waals' contact to another molecule in the crystals are given. Underlined residues form hydrogen bonds with their side-chains between molecules or bind Cd. Bold face numbers indicate main-chain hydrogen bonds to

**Table 5**

*Differences between the three T4 glutaredoxin molecules and the two *E. coli* thioredoxin molecules*

| Molecule       | r.m.s. difference (Å) |                     |                          |                          |        |        |
|----------------|-----------------------|---------------------|--------------------------|--------------------------|--------|--------|
|                | Wild-type<br>mol. B   | Wild-type<br>mol. B | <i>E. coli</i><br>Mutant | <i>E. coli</i><br>Mutant | mol. A | mol. B |
| T4 wild-type   | 0.52                  | 0.28                | 0.86                     | 0.51                     | 1.69   | 1.69   |
| Mol. A         | (87)                  | (71)                | (87)                     | (71)                     | (56)   | (56)   |
| T4 wild-type   |                       |                     | 0.92                     | 0.53                     | 1.80   | 1.80   |
| Mol. B         |                       |                     | (87)                     | (71)                     | (56)   | (56)   |
| Mutant         |                       |                     |                          |                          | 1.69   | 1.85   |
|                |                       |                     |                          |                          | (56)   | (56)   |
| <i>E. coli</i> |                       |                     |                          |                          | 0.66   |        |
| Mol. A         |                       |                     |                          |                          |        | (108)  |

The values are given as r.m.s. differences in Å. The figures in parentheses are the number of superimposed C<sup>α</sup> atoms. Residues 1 to 35, 44 to 56 and 65 to 87 were used in the superposition of the glutaredoxin molecules. For the superposition of glutaredoxin and thioredoxin molecules, residues listed in Table II in Eklund *et al.* (1984) were used. Mol., molecule.

environment in the two molecules. These include Lys13, Arg22, Lys40, Gln81, Arg83 and Glu84, which all have atoms that differ by more than 4 Å between the positions in two of the molecules. All these side-chains have different interactions with neighboring molecules (Table 4). The interaction of the active site in molecule B with neighboring molecules (Table 4) causes the side-chain of Tyr16 to have a different conformation (Fig. 11). The positions of the OH groups differ by 2.8 Å between the two molecules.

#### (g) Temperature factors

In later stages, restrained temperature factors have been refined for wild-type and mutant glutaredoxin. The temperature factors obtained for the α-carbon atoms are shown in Figure 12. The temperature factors differ for the three molecules. Wild-type molecule A generally has the highest temperature factors. The temperature factors for the mutant glutaredoxin are generally lower than for the wild-type molecules, probably due to a tighter packing of molecules in these crystals. Wild-type molecule B and the mutant glutaredoxin molecule have comparable temperature factors, except for residues 38 to 64 and for α3, where in molecule B they are significantly higher.

Residues 57 to 64 have poor electron density and consequently high temperature factors for both wild-type molecules. In the mutant glutaredoxin, the loop is involved in crystal contacts and has a defined conformation and lower temperature factors.

another molecule. For example, Met1 in molecule A is in contact with residue 56 and 58 in another molecule, Met1 in molecule B is in contact with residues 62 (main-chain of Met1 forms a hydrogen bond) and 64 and finally, Met1 in the mutant glutaredoxin is in contact with residues 12 and 40 of neighboring molecules.

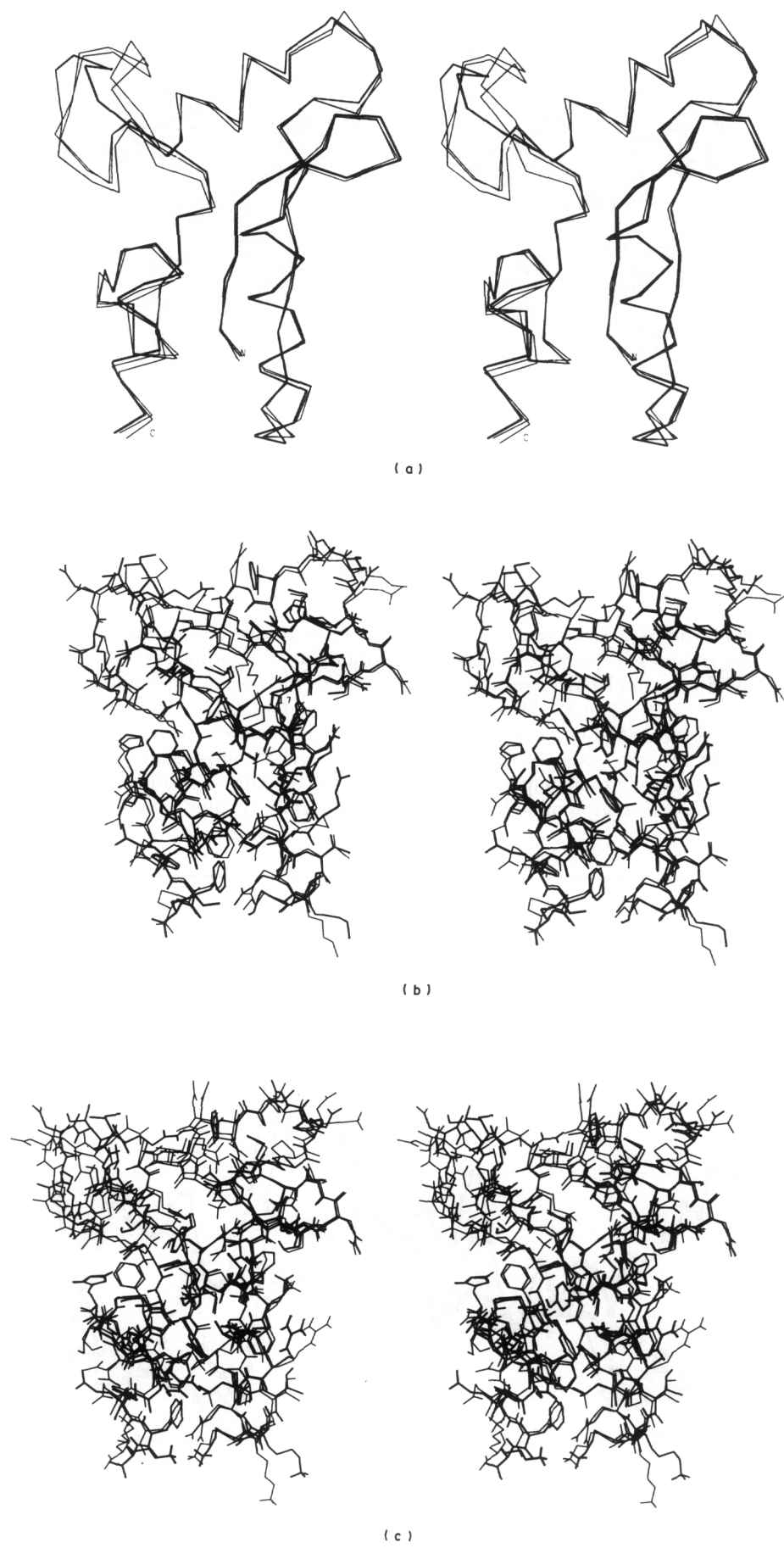
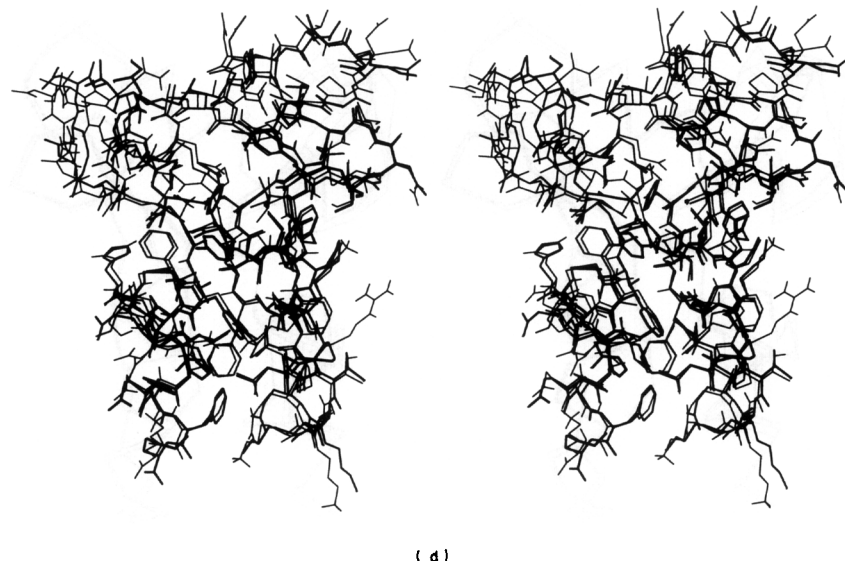


Fig. 11.



**Figure 11.** Comparison between the two native glutaredoxins in the asymmetric unit and the mutant glutaredoxin. (a)  $C^\alpha$  drawing of wild-type T4 glutaredoxin molecule A (in thick lines), molecule B and mutant glutaredoxin. (b) The 2 wild-type molecules with all side-chains. (c) Wild-type molecule A (in thick lines) and the mutant glutaredoxin. (d) Wild-type molecule B (in thick lines) and the mutant glutaredoxin.

There are significant differences in temperature factors for half of the residues in the two independently determined wild-type molecules: residues 8 to 29 ( $\alpha T + \alpha 1$ ), and the region 64 to 83. Due to the packing of the two molecules, the environment of these parts is different in the two cases. In molecule A, residues 8 to 28 are exposed to solvent more or less throughout, while the same region in molecule B

has several interactions with other molecules. Most importantly, residues in the active site area here interact with other molecules. His12 in molecule B is a ligand of Cd2. Tyr16 in this molecule makes several interactions with other molecules. Molecule A has lower temperature factors than the others only for the turn 1 residues since Glu39 in this loop in molecule A binds to Cd2. Similarly, residues

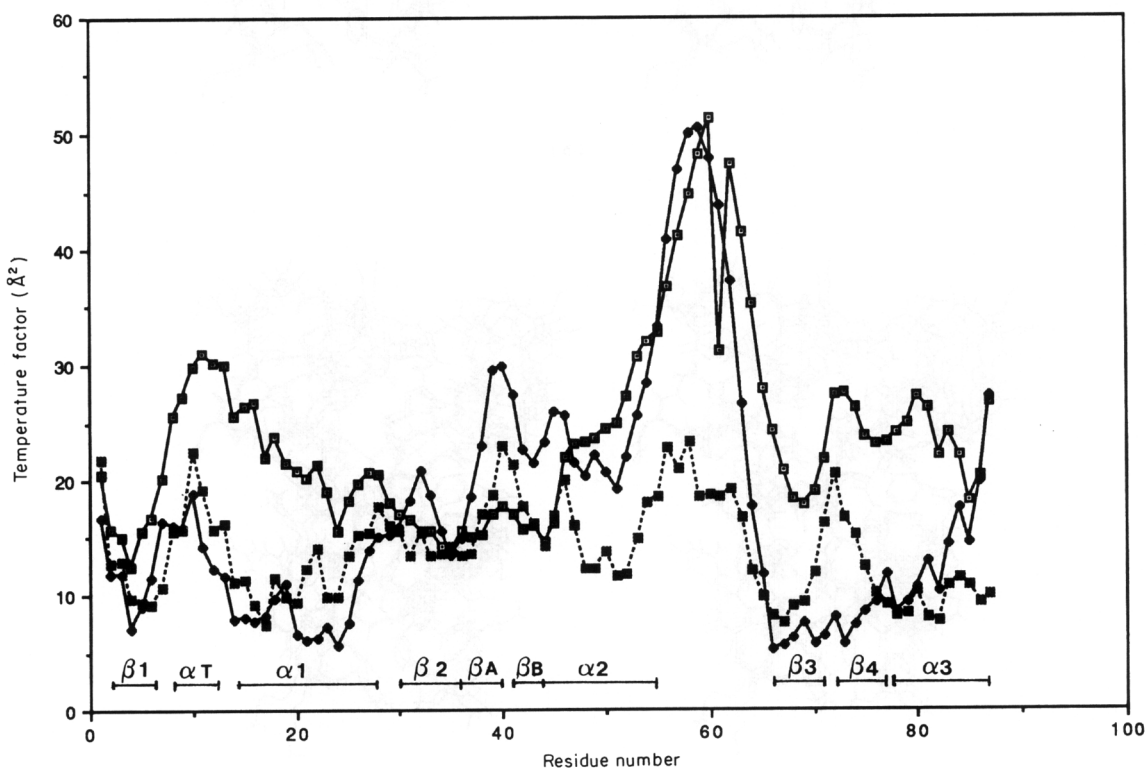


**Figure 12.** Temperature factors. Temperature factors for  $C^\alpha$  atoms in wild-type molecule A (—□—□—), molecule B (◆—◆—) and mutant glutaredoxin (---■---■---). The secondary structure assignments are written below the curves.

**Table 6**  
*Differences in side-chain conformations of the two wild-type molecules of T4 glutaredoxin and the mutant protein*

| Residue | Comment  |
|---------|--|
| Met1    | Different in all three molecules, subunit interactions   |
| Lys3    | Outer atoms differ slightly, diverge outwards  |
| Asn10   | Outer atoms differ slightly  |
| His12   | Differences in $\chi_2$  |
| Lys13   | Different in all three, diverge outwards   |
| Val15   | Different rotamer in the two wild-type molecules   |
| Tyr16   | Significantly different in the two wild-type molecules, different packing interactions   |
| Asp18   | Outer atoms differ for wild-type molecule B  |
| Arg22   | Very different in all three molecules, subunit interactions, the largest difference is 10 Å between atoms in molecule B and the mutant protein |
| Leu23   | Different rotamers in all three molecules, subunit interactions  |
| Lys27   | Outer atoms differ slightly  |
| Lys28   | Very different in all three molecules, especially for the mutant protein, subunit interactions   |
| Gln29   | Differ in wild-type molecule B   |
| Pro30   | Different puckering  |
| Glu32   | Outer atoms differ slightly  |
| Glu39   | Different in all three molecules, subunit interactions   |
| Lys40   | Different in all three molecules   |
| Lys47   | Outer atoms differ slightly  |
| Arg57   | Different in all three molecules   |
| Leu63   | Different in all three molecules   |
| Asp72   | Different in all three molecules, subunit interactions   |
| Gly73   | The oxygen atom points differently in all three molecules  |
| Ser74   | Different $\chi_1$ -torsion in all three molecules   |
| Asp80   | Different in all three molecules, especially the mutant protein, subunit interactions  |
| Gln81   | Different in wild-type molecule B, subunit interactions  |
| Arg83   | Different in all three molecules, subunit interactions   |
| Glu84   | Different in all three molecules, subunit interactions   |
| Lys87   | Very different in all three molecules, subunit interactions  |

around turn 4 have significantly lower temperature factors in molecule B than for the other molecules due to binding of Asp72 to Cd2.

#### (h) Alternative side-chain conformations

For the mutant glutaredoxin, the resolution is high enough to see alternative conformations for the side-chains. From the final  $2|F_o| - |F_c|$  and  $|F_o| - |F_c|$  maps it was evident that several side-chains have alternative conformations. Certain extended surface side-chains, e.g. Lys13, Lys40 and Glu46 have equally weighted electron density for each conformer. Pro30 has electron density corresponding to both pucker conformations of the ring. Tyr85 occupies two positions in the same ring plane (Fig. 4), similar to Tyr29 in the highly refined crambin structure (Smith *et al.*, 1986). The most unexpected multiple conformer is Leu55, where the

side-chain is turned by about  $10^\circ$  giving rise to two conformations (Fig. 4).

#### (i) Solvent structure

Most of the exposed polar main-chain atoms of the molecule are hydrogen bonded to ordered water molecules. For the wild-type glutaredoxin, 222 water molecules have been included, and for the mutant glutaredoxin, 140 water molecules (Fig. 13). In 12 cases, main-chain carbonyl oxygen atoms in the mutant protein make hydrogen bonds to two water molecules. In all, 15 of the exposed polar main-chain atoms do not make a hydrogen bond to any ordered water molecule.

In the difference Fourier map between reduced and oxidized mutant glutaredoxin, a strong negative peak appeared in the solvent region (M.I., P.N. & H.E., unpublished results). Analysis of the electron density of this region suggests that it should correspond to a Mes-buffer molecule with its sulfate moiety corresponding to the strong negative peak. A Mes-buffer molecule fits well into the density in the oxidized mutant glutaredoxin (Fig. 13). Its oxygen atoms form hydrogen bonds with N65 and a water molecule. The ring oxygen atom of Mes is hydrogen bonded to the side-chain of Gln60. This buffer molecule is probably not present in the crystals with reduced glutaredoxin because of electrostatic repulsion of the charged Cys14.

#### (j) The active site disulfide bridge

The disulfide bridge which is responsible for the redox activity of the protein is formed between cysteines 14 and 17. These residues form the first turn of  $\alpha 1$ . The residues in the ring structure formed by the disulfide also include Val15 and Tyr16. In relation to the pleated sheet, the active site is located close to the carboxyl end of  $\beta 1$  and  $\beta 2$  and the amino end of  $\beta 3$ . The sheet here begins to widen and extend into loop regions. From the sheet side, the residues closest to the disulfide bridge are Phe33 of strand  $\beta 2$ , Pro66 at the start of  $\beta 3$  and Tyr7 just at the end of  $\beta 1$ .

One side of the S-S bridge is covered by  $\alpha T$ ,  $\alpha 1$  and  $\beta 2$  (particularly residues 8, 18, 21 and 33). There is also a well-ordered water molecule between Lys21 and Asp8. The sulfur atoms are also covered from this side by the  $\beta$ -carbon atoms of the cysteine residues. The S-S bridge is accessible from the opposite direction through a cleft (Fig. 14). The central part of this cleft is devoid of charged residues. Some hydrophobic residues, Met65 and Pro66 and polar residues, Tyr7 and Tyr16, constitute the walls of this cleft. At the ends of the cleft there are charged residues, His12 and Asp80. The sulfur atom of Cys14 is at the bottom of the cleft and is accessible to solvent (Table 7). Lys13 points away from the cleft.

The sulfur atom of Cys17 is buried in the inner part of the helix turn and has no surface area accessible to water (Table 7). The sulfur atoms are

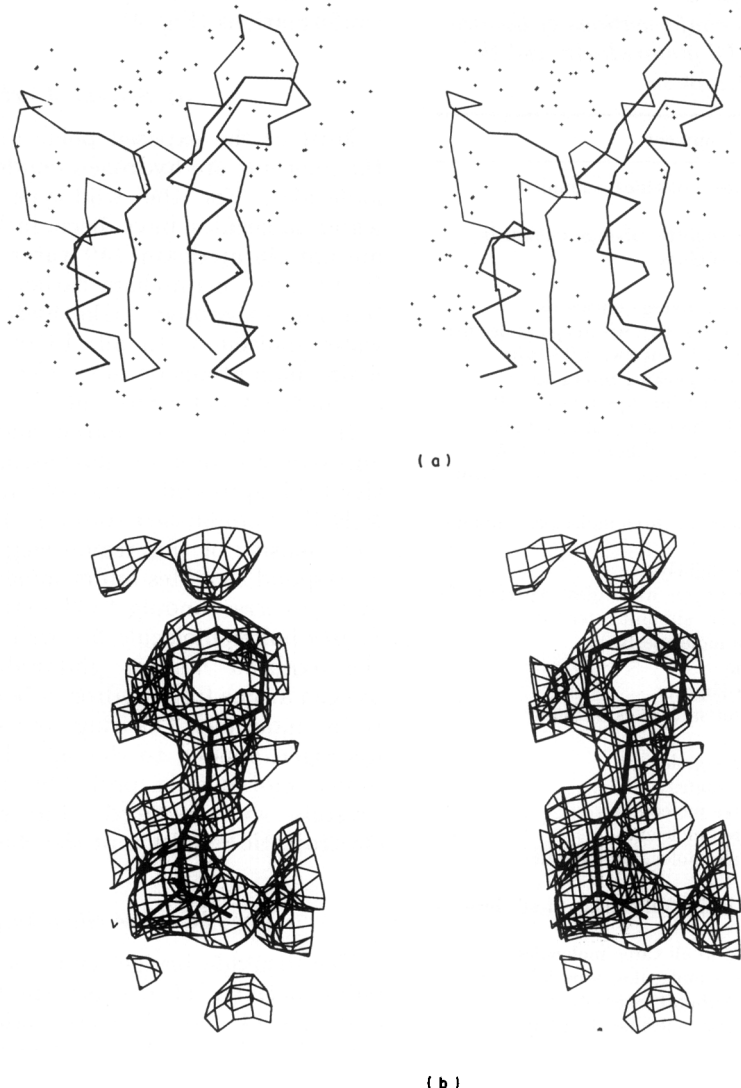


**Figure 13.** Solvent and buffer molecules around T4 glutaredoxin. Water molecules in the mutant glutaredoxin in (a) C<sup>α</sup> chain. (b) The electron density corresponding to the Mes molecule. The  $2|F_o| - |F_c|$  map is calculated without contribution of the Mes molecule contoured at 0.7σ.

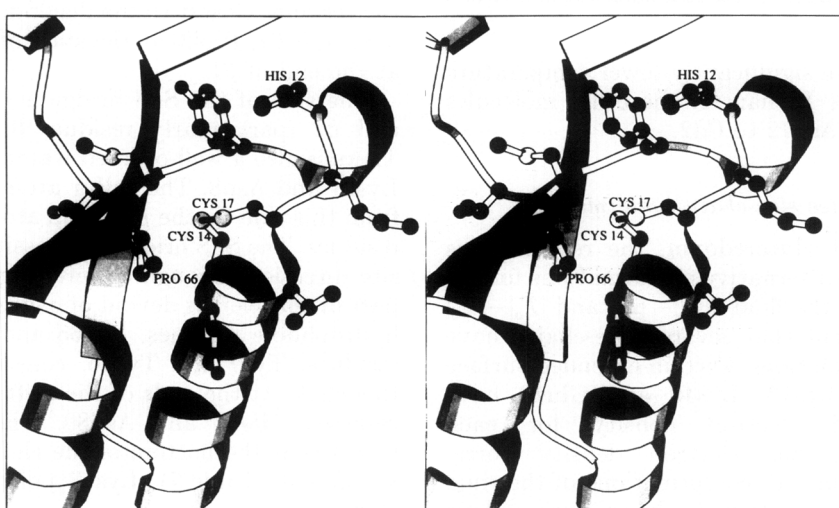


**Figure 14.** Active site. A MolScript view (Kraulis, 1991) of the active site in wild-type glutaredoxin molecule A with the redox-active disulfide bridge at the center. The side-chains of Tyr7, His12, Tyr16, Thr64 form a cleft, which has been suggested to bind glutathione (Nikkola et al., 1991).

**Table 7**  
Accessible surface area for residues in the active site area

|       | N              | C              | O              | C <sup>a</sup> | C <sup>b</sup> | C <sup>c</sup> | C <sup>d</sup> | C <sup>e</sup> | C <sup>f</sup> | C <sup>g</sup> | O <sup>h</sup> |
|-------|----------------|----------------|----------------|----------------|----------------|----------------|----------------|----------------|----------------|----------------|----------------|
|       | O <sup>y</sup> | N <sup>d</sup> | C <sup>d</sup> | C <sup>e</sup> | N <sup>e</sup> | N <sup>f</sup> |                |                |                |                |                |
|       | S <sup>y</sup> | O <sup>d</sup> | N <sup>d</sup> |                |                |                |                |                |                |                |                |
| Gly6  | 0              | 0              | 0              | 0              |                |                |                |                |                |                |                |
| Tyr7  | 0              | 0              | 0              | 0              | 0              | 0              | 0              | 0              | 14             | 0              | 16             |
| Ser9  | 3              | 0              | 9              | 0              | 12             | 0              |                |                |                |                |                |
| His12 | 0              | 0              | 0              | 4              | 0              | 0              | 12             | 1              | 48             | 24             |                |
| Lys13 | 6              | 1              | 11             | 0              | 22             | 27             | 0              | 40             |                | 49             |                |
| Cys14 | 0              | 0              | 0              | 6              | 0              | 6              |                |                |                |                |                |
| Val15 | 2              | 0              | 0              | 0              | 6              | 47             | 39             |                |                |                |                |
| Tyr16 | 1              | 0              | 0              | 0              | 0              | 0              | 14             | 0              | 26             | 26             | 10             |
| Cys17 | 0              | 0              | 0              | 0              | 0              | 0              |                |                |                |                |                |
| Asp18 | 0              | 1              | 4              | 1              | 19             | 13             | 5              | 17             |                |                |                |
| Asn19 | 0              | 0              | 0              | 0              | 0              | 4              | 20             | 13             |                |                |                |
| Ala20 | 0              | 0              | 0              | 0              | 0              |                |                |                |                |                |                |
| Lys21 | 0              | 0              | 0              | 0              | 10             | 0              | 5              | 23             |                | 18             |                |
| Met65 | 4              | 0              | 0              | 0              | 5              | 7              | 0              | 1              |                |                |                |
| Pro66 | 0              | 0              | 0              | 0              | 0              | 0              | 0              |                |                |                |                |

|       | N              | C              | O              | C <sup>a</sup> | C <sup>b</sup> | C <sup>c</sup> | C <sup>d</sup> | C <sup>e</sup> | C <sup>f</sup> | C <sup>g</sup> | O <sup>h</sup> |
|-------|----------------|----------------|----------------|----------------|----------------|----------------|----------------|----------------|----------------|----------------|----------------|
|       | O <sup>y</sup> | N <sup>d</sup> | C <sup>d</sup> | C <sup>e</sup> | N <sup>e</sup> | N <sup>f</sup> |                |                |                |                |                |
|       | S <sup>y</sup> | O <sup>d</sup> | N <sup>d</sup> |                |                |                |                |                |                |                |                |
| Gly6  | 0              | 0              | 0              | 0              |                |                |                |                |                |                |                |
| Tyr7  | 0              | 0              | 0              | 0              | 0              | 0              | 0              | 0              | 14             | 0              | 16             |
| Ser9  | 3              | 0              | 9              | 0              | 12             | 0              |                |                |                |                |                |
| His12 | 0              | 0              | 0              | 4              | 0              | 0              | 12             | 1              | 48             | 24             |                |
| Lys13 | 6              | 1              | 11             | 0              | 22             | 27             | 0              | 40             |                | 49             |                |
| Cys14 | 0              | 0              | 0              | 6              | 0              | 6              |                |                |                |                |                |
| Val15 | 2              | 0              | 0              | 0              | 6              | 47             | 39             |                |                |                |                |
| Tyr16 | 1              | 0              | 0              | 0              | 0              | 0              | 14             | 0              | 26             | 26             | 10             |
| Cys17 | 0              | 0              | 0              | 0              | 0              | 0              |                |                |                |                |                |
| Asp18 | 0              | 1              | 4              | 1              | 19             | 13             | 5              | 17             |                |                |                |
| Asn19 | 0              | 0              | 0              | 0              | 0              | 4              | 20             | 13             |                |                |                |
| Ala20 | 0              | 0              | 0              | 0              | 0              |                |                |                |                |                |                |
| Lys21 | 0              | 0              | 0              | 0              | 10             | 0              | 5              | 23             |                | 18             |                |
| Met65 | 4              | 0              | 0              | 0              | 5              | 7              | 0              | 1              |                |                |                |
| Pro66 | 0              | 0              | 0              | 0              | 0              | 0              |                |                |                |                |                |

Residues within 10 Å from the disulfide bridge are included. The accessible surface area is calculated according to Lee & Richards (1971).

in van der Waals' contact to main-chain atoms of residues 6, 7 and 17 and side-chain atoms of Met65 and Pro66 (Table 8).

There are hydrogen bonds between the main-chain nitrogen atoms of residues 7 and 17 and the sulfur atoms of Cys17 and Cys14, respectively. The bond lengths are 3.3 to 3.6 Å, comparable to cysteinyl hydrogen bonds found in iron-sulfur proteins (Adman *et al.*, 1975). Only one hydrogen bond of this type is found in *E. coli* thioredoxin, where Cys32 is involved in a hydrogen bond with the main-chain N35, while Cys35 is devoid of any such interaction (Katti *et al.*, 1990). Hydrogen bonds to cysteine sulfur atoms should influence the redox potential of the protein by stabilizing the negative charged thiolate form of the cysteine residues.

The reactivity of a cysteine residue is dependent on its environment. The unusual reactivity of papain and other thiol proteases is correlated to a neighboring charged His (Lewis *et al.*, 1976). The p*K*<sub>a</sub> of the active site cysteine in papain has been estimated to be 3.3. Cys32 and Cys35 in *E. coli* thioredoxin have p*K*<sub>a</sub> values of 6.8 and 8.7, respectively (Kallis & Holmgren, 1980). For glutaredoxins, the p*K*<sub>a</sub> of the exposed active site Cys has been estimated to be lower than for thioredoxins (Björnberg, 1990; Sandberg *et al.*, 1991). The p*K*<sub>a</sub> for the active site cysteine residues in T4 glutaredoxin has not yet been determined, but the exposed Cys14 should be expected to have a low p*K*<sub>a</sub> value, as do Cys residues in the other glutaredoxins. There are no charged residues close to the active site cysteines (Table 9). Only three charged residues are closer than 8 Å to any of the sulfur atoms: Asp81, Lys21 and His12. Of these, Asp18 is

**Table 8**  
Atoms in contact with the cysteine sulfur atoms

|                 | Atom | Distances (Å)        |                      |                     |
|-----------------|------|----------------------|----------------------|---------------------|
|                 |      | Wild-type molecule A | Wild-type molecule B | Mutant glutaredoxin |
| <b>A. Cys14</b> |      |                      |                      |                     |
| Cys17           | SG   | 2.03                 | 2.00                 | 2.03                |
|                 | N    | 3.4                  | 3.3                  | 3.4                 |
|                 | CA   | 3.8                  | 3.8                  | 3.8                 |
|                 | CB   | 3.1                  | 3.1                  | 3.1                 |
| Met65           | O    | 4.4                  | 4.4                  | 3.8                 |
|                 | CB   | 4.3                  | 3.9                  | 4.4                 |
| Water           | O    | 3.8                  |                      | 3.8                 |
| Water           | O    |                      |                      | 3.7                 |
| <b>B. Cys17</b> |      |                      |                      |                     |
| Gly6            | CA   | 3.8                  | 3.9                  | 3.9                 |
| Tyr7            | N    | 3.5                  | 3.5                  | 3.6                 |
|                 | O    | 3.9                  | 3.7                  | 4.2                 |
| Cys14           | CB   | 3.2                  | 3.1                  | 3.0                 |
|                 | SG   | 2.03                 | 2.00                 | 2.03                |
| Met65           | CB   | 4.0                  | 4.2                  | 4.0                 |
| Pro66           | N    | 3.8                  | 4.1                  | 3.9                 |
|                 | CB   | 3.7                  | 4.1                  | 4.1                 |
|                 | CD   | 3.8                  | 4.0                  | 4.0                 |

All atoms closer than 4 Å are included.

closest and should perturb the p*K*<sub>a</sub> value upward. Thus, the side-chains do not seem to contribute to the lowering of p*K*<sub>a</sub> of the cysteine residues; main-chain atoms are probably much more important. However, charged side-chains are important in interactions with glutathione and thioredoxin reductase, as has been demonstrated by site-directed mutagenesis. His12, Lys13, Lys21 and Asp80 have been substituted by uncharged side-chains and they show significant changes in activity (Nikkola *et al.*, 1991, and unpublished results).

#### (k) The disulfide bridge conformation

Disulfide bridges often connect two parts of a protein distant in sequence. For redox-active disulfide proteins the cysteine residues are often

**Table 9**  
Distances between charged residues and the cysteine sulfur atoms of the active site (Å)

| Residue | Atom            | Cys14 |      |        | Cys17 |      |        |
|---------|-----------------|-------|------|--------|-------|------|--------|
|         |                 | A     | B    | Mutant | A     | B    | Mutant |
| Asp8    | O <sup>δ2</sup> | 10.1  | 9.8  | 10.0   | 9.5   | 9.1  | 9.5    |
| His12   | N <sup>ε2</sup> | 7.3   | 7.6  | 7.0    | 8.6   | 9.0  | 8.2    |
| Lys13   | N <sup>ε</sup>  | 10.8  | 10.3 | 10.0   | 12.5  | 11.6 | 11.4   |
| Asp18   | O <sup>δ2</sup> | 6.4   | 6.4  | 6.5    | 6.5   | 6.2  | 6.2    |
| Lys21   | N <sup>ε</sup>  | 8.1   | 8.3  | 8.7    | 6.8   | 6.9  | 7.4    |
| Arg22   | N <sup>η2</sup> | 9.8   | 12.4 | 10.6   | 9.9   | 12.7 | 10.5   |
| Lys40   | N <sup>ε</sup>  | 13.9  | 15.9 | 16.9   | 15.0  | 16.2 | 17.7   |
| Arg57   | N <sup>η2</sup> | 14.6  | 15.7 | 16.3   | 14.5  | 15.8 | 16.0   |
| His75   | N <sup>ε2</sup> | 13.6  | 13.8 | 13.8   | 12.6  | 12.9 | 12.7   |
| Asp80   | O <sup>δ2</sup> | 12.5  | 12.4 | 14.4   | 12.9  | 12.9 | 14.6   |
| Arg83   | N <sup>η2</sup> | 14.3  | 14.1 | 13.2   | 14.5  | 14.5 | 13.3   |

**Table 10**  
*Torsion angles for the disulfide bridge in T4 glutaredoxin, in the mutant protein and E. coli thioredoxin*

|                                  | 1st cysteine    |                 |                 | 2nd cysteine    |                 |  | S-S<br>(Å) | C <sup>α</sup> -C <sup>α</sup><br>(Å) | C <sup>β</sup> -C <sup>β</sup><br>(Å) |
|----------------------------------|-----------------|-----------------|-----------------|-----------------|-----------------|--|------------|---------------------------------------|---------------------------------------|
|                                  | $\chi_1$<br>(°) | $\chi_2$<br>(°) | $\chi_3$<br>(°) | $\chi_1$<br>(°) | $\chi_2$<br>(°) |  |            |                                       |                                       |
| <b>A. Native T4 glutaredoxin</b> |                 |                 |                 |                 |                 |  |            |                                       |                                       |
| Molecule A                       | -173            | -141            | 58              | -66             | 89              |  | 2.03       | 5.3                                   | 3.6                                   |
| Molecule B                       | -174            | -142            | 67              | -55             | 80              |  | 2.00       | 5.2                                   | 3.6                                   |
| <b>B. Mutant T4 glutaredoxin</b> |                 |                 |                 |                 |                 |  |            |                                       |                                       |
| CGPC                             | -175            | -146            | 67              | -59             | 82              |  | 2.03       | 5.2                                   | 3.6                                   |
| <b>C. E. coli thioredoxin</b>    |                 |                 |                 |                 |                 |  |            |                                       |                                       |
| Molecule A                       | 165             | -132            | 81              | -62             | 79              |  | 2.09       | 5.2                                   | 3.7                                   |
| Molecule B                       | 167             | -136            | 72              | -62             | 82              |  | 2.05       | 5.2                                   | 3.6                                   |

separated by two residues as in glutaredoxins, thiol-transferases, thioredoxins and thioredoxin reductase, while for another group of redox proteins, the cysteine pairs are separated by five residues, as for glutathione reductase and mercuric ion reductase. For glutaredoxins and thioredoxins, the  $\alpha$ -carbon atoms of the cysteine residues are 5.2 to 5.3 Å from each other (Table 10). The  $\beta$ -carbon atoms are in van der Waals' contact on the same side of the sulfur atoms.

The torsion angles for the cysteine residues in all three glutaredoxin molecules are close to common groups of angles for disulfide cysteines (Thornton, 1981; Richardson, 1981). Cys14 is extended with the torsion angles  $\chi_1 = -174^\circ (\pm 1^\circ)$  and  $\chi_2 = -143^\circ (\pm 3^\circ)$ , similar to disulfide bridges in immunoglobulins (Thornton, 1981). Cys17 has common side-chain torsion angles with  $\chi_1 = -60^\circ (\pm 6^\circ)$  and  $\chi_2 = 84^\circ (\pm 5^\circ)$ . The torsion angle around the S-S bridge is  $64^\circ (\pm 6^\circ)$ . The torsion angles are similar to those of *E. coli* thioredoxin (Table 10). The torsion angle around the disulfide bridge in T4 glutaredoxin is smaller than the commonly found cluster around  $90^\circ$  and also slightly smaller than in *E. coli* thioredoxin, for which the average value for the two molecules is  $76^\circ$ .

The overall conformation of the active site disulfide bridge of glutaredoxin is different from that of glutathione reductase, mercuric ion reductase and lipoamide reductase, where the cysteine residues are separated by five residues (Karplus & Schulz, 1987; Schiering *et al.*, 1991; Mattevi *et al.*, 1991). While the glutaredoxin disulfide can be regarded as having the cysteine residues roughly in *cis* conformation around the disulfide bond, the cysteines of the glutathione reductase group are roughly in *trans* conformation. The torsion angles for the disulfide bridge in these proteins are about  $-120^\circ$ .

#### (I) Highly conserved residues

The five known glutaredoxin sequences have a characteristic pattern of conserved residues

**Table 11**  
*Highly conserved residues in glutaredoxin sequences*

| Residue | Organism<br>in which<br>residue<br>differs | Residue in<br>divergent<br>organism | Comment  |
|---------|--|-------------------------------------|--|
| Lys3    | <i>E. coli</i>                             | Thr                                 | In the strand $\beta$ A, close to Glu32                            |
| Val4    | —  | —                                   | Hydrophobic core 1, proximally located in strand $\beta$ A         |
| Cys14   | —  | —                                   | Active site cysteine   |
| Pro15   | T4   | Val                                 | At the active site   |
| Tyr16   | Pig  | Phe                                 | At the active site   |
| Cys17   | —  | —                                   | Active site cysteine   |
| Leu23   | Rabbit                                     | Ile                                 | $\alpha$ 1, hydrophobic core 1                                     |
| Leu24   | <i>E. coli</i>                             | Ala                                 | $\alpha$ 1, hydrophobic core 1                                     |
| Leu28   | T4   | Lys                                 | End of helix $\alpha$ 1 which is shorter in T4 glutaredoxin        |
| Glu32   | <i>E. coli</i>                             | Gln                                 | At the surface of strand $\beta$ B, close to Lys3                  |
| Phe33   | <i>E. coli</i>                             | Tyr                                 | Close to disulfide bridge on the shielded side, hydrophobic core 1 |
| Val34   | T4   | Ile                                 | Hydrophobic core 2   |
| Asp35   | T4   | Asn                                 | At the surface   |
| Ile36   | —  | —                                   | Hydrophobic core 2   |
| Ala38   | T4   | Pro                                 | —  |
| Glu48   | —  | —                                   | At the surface   |
| Leu51   | —  | —                                   | Hydrophobic core 2   |
| Gly56   | —  | —                                   | End of helix $\alpha$ 2  |
| Thr64   | —  | —                                   | Glutathione binding cleft  |
| Val65   | T4   | Met                                 | Close to active site, hydrophobic core 2                           |
| Pro66   | —  | —                                   | cis-Pro, in van der Waals' contact to disulfide bridge             |
| Val68   | <i>E. coli</i>                             | Ile                                 | Hydrophobic core 1   |
| Phe69   | —  | —                                   | Hydrophobic core 2   |
| Ile76   | —  | —                                   | Hydrophobic core 1   |
| Gly77   | —  | —                                   | Close to active site   |
| Gly78   | —  | —                                   | Close to active site   |
| Asp81   | T4   | Gln                                 | N-Terminal of $\alpha$ 3   |
| Leu82   | <i>E. coli</i>                             | Phe                                 | Hydrophobic core 1   |
| Leu91   | T4   | —                                   | After the carboxyl end, T4 glutaredoxin shorter                    |

Positions are included where the residue is the same in at least all sequences but one.

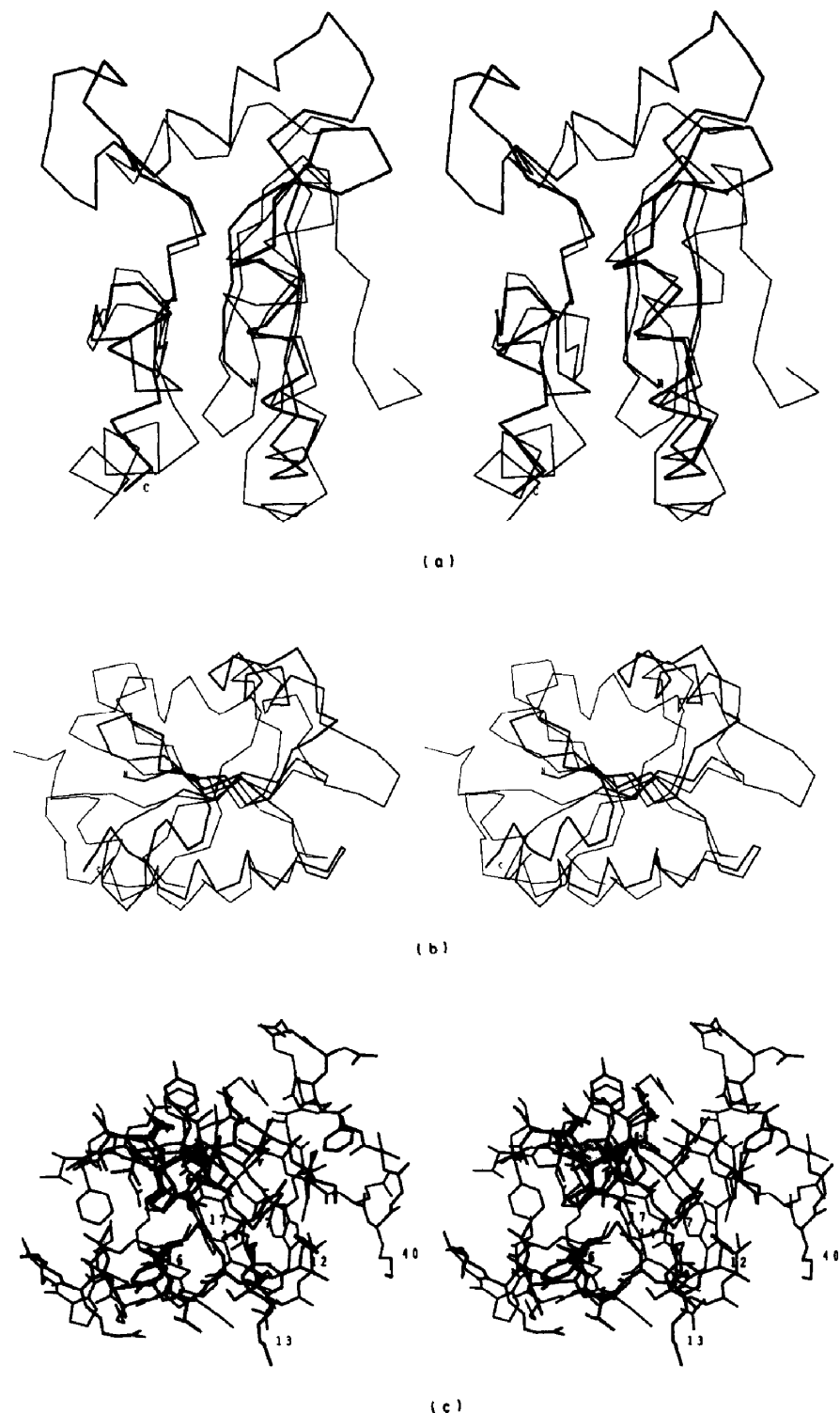


**Figure 15.** Comparison between T4 glutaredoxin and *E. coli* thioredoxin. (a) Main-chain conformation of T4 glutaredoxin (thick lines) and *E. coli* thioredoxin superimposed by  $C^\alpha$  atoms of residues in the common core of the 2 molecules as defined in Table 1 in Eklund *et al.* (1984). (b) A view perpendicular to that in (a). (c) View of the active site in the 2 molecules superimposed. T4 glutaredoxin in thick lines.

(Nikkola *et al.*, 1991) which differs distinctly from the pattern of conserved residues in the thioredoxins (Eklund *et al.*, 1991). The conserved residues are listed in Table 11.

Residues around the *cis*-Pro66 and Gly77-Gly78 in the bends at the active site are conserved. These residues were included in the uncharged surface at

the active site which had earlier been proposed to be important for activity and present in T4 glutaredoxin, *E. coli* glutaredoxin and thioredoxins from *E. coli* and *Corynebacterium nephridii* (Eklund *et al.*, 1984). This surface also includes residues 15 and 16, which are highly homologous in all the glutaredoxins. Close to the active site at the end of the

suggested glutathione binding cleft, there is a conserved aspartic acid in the first turn of  $\alpha$ 3, residue 80 or 81. The replacement of Asp80 with a Ser reduces the glutathione activity (Nikkola *et al.*, 1991).

Several of the internal hydrophobic residues Val4, Ile36, Leu51, Phe71 and Ile76 are completely conserved, while Leu23, Leu24, Val34, Val65, Val68 and Leu82 are highly conserved.

#### (m) Comparison with *E. coli* thioredoxin

The similarities between T4 glutaredoxin and *E. coli* thioredoxin were early recognized (Söderberg *et al.*, 1978). A more detailed comparison was also made at an intermediate stage of the refinement when the *E. coli* thioredoxin structure was in the early stages of refinement, while the T4 glutaredoxin was reasonably well refined. Both structures have now been refined at high resolution and a more detailed comparison is possible. The identity between structures has only increased slightly relative to the earlier study (an r.m.s. difference of 1.7 Å instead of 1.8 Å for the 56 residues in the core of the molecule).

The main difference between the two proteins is the location of the disulfide bridge (Fig. 15). In thioredoxin, the active site residues are located as a protruding part of an otherwise compact disc structure. In glutaredoxin, the active site is located more centrally in the base of a funnel spawned from long loops. Three loops are longer at the active site side of the molecule than in thioredoxin, residues 10 to 12, 38 to 44 and 53 to 65. The disulfide bridge is thus not located in any protruding part of the glutaredoxin, as in *E. coli* thioredoxin, but resides instead in a largely occluded cleft.

Another distinction is that there is no pronounced active site cleft in the thioredoxin molecule. The disulfide bridge is on the shielded side of the protrusion with only a shallow depression beside the exposed cysteine residue. In the glutaredoxin, there is a pronounced cleft formed by residues in the surrounding loops and Tyr16 (Fig. 14). The active site in thioredoxin seems more suited to approach surface cysteine residues in proteins, while the cleft in the glutaredoxin seems more suitable as a binding site for a small molecule such as glutathione. However, the glutaredoxin molecule must be able to reduce the active site cysteine residues in ribonucleotide reductase, which is its main metabolic function.

T4 glutaredoxin and *E. coli* thioredoxin enjoy certain functionalities in common. Both molecules are reduced by thioredoxin reductase and, while T4 glutaredoxin can reduce *E. coli* ribonucleotide reductase, it does so less efficiently than does *E. coli* thioredoxin. At the active site protrusion in thioredoxins, there is a conserved tryptophan, number 31, in *E. coli* thioredoxin. In glutaredoxin, the position of the side-chain of this residue corresponds to two residues in glutaredoxin: His12 and Tyr7 (Fig. 15(c)) that form a similarly shaped surface which may be involved in the enzyme interactions.

#### (n) The mutant glutaredoxin

Mutation of the two residues between the two redox active cysteines in T4 glutaredoxin, Val15 and Tyr16, to Gly and Pro as in *E. coli* thioredoxin, has increased the activity of the mutant protein with *E. coli* ribonucleotide reductase relative to the activity of *E. coli* thioredoxin (Joelson *et al.*, 1990).

The structure of this mutant glutaredoxin described here shows that the main-chain and cysteine conformations are very similar to those of wild-type glutaredoxin. This suggests that the main cause of the difference in activity between wild-type and mutant glutaredoxin with *E. coli* ribonucleotide reductase is due to the protruding tyrosine side-chain in the wild-type protein. The tyrosine side-chain does not harm the reduction of T4 ribonucleotide reductase by glutaredoxin, its physiological reaction (Joelson *et al.*, 1990). On the other hand, the cleft formed by the tyrosine side-chain seems to be essential for the reduction by glutathione (Nikkola *et al.*, 1991).

The redox equilibrium between NADP and thioredoxin or glutaredoxin is strongly shifted towards reduced protein. However, there is an order of magnitude difference between the equilibrium constant for T4 glutaredoxin and *E. coli* thioredoxin, with glutaredoxin being the more markedly reduced. The redox potential of the mutant glutaredoxin is more similar to that of *E. coli* thioredoxin. One possible reason for this is that these properties are related to the S-S torsion angle. In the wild-type glutaredoxin, the active site is exposed to the surface only in molecule A. The torsion angles for molecule B may be influenced by packing interactions. If molecule B is excluded, the S-S torsion angle in the wild-type glutaredoxin deviates most from the ideal 90°, while thioredoxin deviates less, and the mutant glutaredoxin is intermediary between the two. The less relaxed conformation of the disulfide bridge of glutaredoxin may explain the differences in redox properties.

This work was supported by the Swedish Natural Science Research Council and the Swedish National Board for Technical Development. We are indebted to Professor Carl-Ivar Brändén, Uppsala, Professor Alwyn Jones, Uppsala and Professor Britt-Marie Sjöberg, Stockholm for their contributions in the earlier parts of the project. We also thank Professor Robert Diamond, Cambridge, England and Professor Robert Huber for access to computer graphics at a very early stage of the work. We are grateful to Michael Fothergill for linguistic corrections of the manuscript.

#### References

- Adman, E., Watenpaugh, K. D. & Jensen, L. H. (1975). NH $\cdots$ S hydrogen bonds in *Peptococcus aerogenes* ferredoxin, *Clostridium pasteurianum* rubredoxin, and *Cromatium* high potential iron protein. *Proc. Nat. Acad. Sci., U.S.A.* **72**, 4854–4858.
- Baker, E. N. & Hubbard, R. E. (1984). Hydrogen bonding in globular proteins. *Prog. Biophys. Mol. Biol.* **44**, 97–179.

- Bennett, W. S. & Huber, R. (1984). Structural and functional aspects of domain motions in proteins. *CRC Crit. Rev. Biochem.* **15**, 291–384.
- Berglund, O. & Sjöberg, B.-M. (1970). A thioredoxin induced by bacteriophage T4. *J. Biol. Chem.* **245**, 6030–6035.
- Björnberg, O. (1990). Licentiate thesis. Karolinska Institute, Stockholm, Sweden.
- Black, S., Harte, E. M., Hudson, B. & Wartofsky, L. A. (1960). A specific enzymatic reduction of L(–) methionine sulfoxide and a related nonspecific reduction of disulfides. *J. Biol. Chem.* **235**, 2910–2916.
- Blum, M., Metcalf, P., Harrison, S. C. & Wiley, D. C. (1987). A system for collection and on-line integration of X-ray diffraction data from a multiwire area detector. *J. Appl. Crystallogr.* **20**, 235–242.
- Borden, K. L. B. & Richards, F. M. (1990a). Folding kinetics of phage T4 thioredoxin. *Biochemistry*, **29**, 3071–3077.
- Borden, K. L. B. & Richards, F. M. (1990b). Folding of the reduced form of the thioredoxin from bacteriophage T4. *Biochemistry*, **29**, 8207–8210.
- Brünger, T. A., Kuriyan, J. & Karplus, M. (1987). Crystallographic R factor refinement by molecular dynamics. *Science*, **235**, 458–460.
- Chothia, C., Levitt, M. & Richardson, D. (1977). Structure of proteins: packing of  $\alpha$ -helices and pleated sheets. *Proc. Nat. Acad. Sci., U.S.A.* **74**, 4130–4134.
- Cséke, C. & Buchanan, B. B. (1986). Regulation of formation and utilization of photosynthate in leaves. *Biochim. Biophys. Acta*, **853**, 43–63.
- Diamond, R. (1982). Bilder: an interactive graphics program for biopolymers. In *Computational Crystallography* (Sayre, D., ed.), pp. 318–325, Oxford University Press, Oxford.
- Dyson, H. J., Gippert, G. P., Case, D. A., Holmgren, A. & Wright, P. E. (1990). Three-dimensional solution structure of the reduced form of *Escherichia coli* thioredoxin determined by nuclear magnetic resonance spectroscopy. *Biochemistry*, **29**, 4129–4136.
- Eklund, H., Cambillau, C., Sjöberg, B.-M., Holmgren, A., Jörnvall, H., Höög, J.-O. & Brändén, C.-I. (1984). Conformational and functional similarities between glutaredoxin and thioredoxins. *EMBO J.* **3**, 1443–1449.
- Eklund, H., Gleason, F. K. & Holmgren, A. (1991). Structural and functional relations among thioredoxins of different species. *Proteins*, **11**, 13–28.
- Forman-Kay, J. D., Clore, G. M., Wingfield, P. T., Gronenborn, A. M. (1991). High-resolution three-dimensional structure of reduced recombinant human thioredoxin in solution. *Biochemistry*, **30**, 2685–2698.
- Hendrickson, W. A. & Konnert, J. H. (1980). Incorporation of stereochemical information into crystallographic refinement. In *Computing in Crystallography* (Diamond, R., Rameseshan, S. & Venkatesan, K., eds), pp. 13.01–13.23, Bangalore, India.
- Holmgren, A. (1978). Glutathione-dependent enzyme reactions of the phage T4 ribonucleotide reductase system. *J. Biol. Chem.* **253**, 7224–7430.
- Holmgren, A. (1985). Thioredoxin. *Annu. Rev. Biochem.* **54**, 237–271.
- Holmgren, A. (1989). Thioredoxin and glutaredoxin systems. *J. Biol. Chem.* **264**, 13963–13966.
- Holmgren, A., Söderberg, B.-O., Eklund, H. & Brändén, C.-I. (1975). Three-dimensional structure of *E. coli* thioredoxin-S<sub>2</sub> to 2.8 Å resolution. *Proc. Nat. Acad. Sci., U.S.A.* **72**, 2305–2309.
- Höög, J.-O., Jörnvall, H., Holmgren, A., Carlquist, M. & Persson, M. (1983). The primary structure of *Escherichia coli* glutaredoxin. Distant homology with thioredoxins in a superfamily of small proteins with a redox active cystine disulfide/cysteine dithiol. *Eur. J. Biochem.* **136**, 223–232.
- Jack, A. & Levitt, M. (1978). Refinement of large structures by simultaneous minimization of energy and R-factor. *Acta Crystallogr. sect. A*, **34**, 931–935.
- Joelson, T., Sjöberg, B.-M. & Eklund, H. (1990). Modifications of the active center of T4 thioredoxin by site-directed mutagenesis. *J. Biol. Chem.* **265**, 3183–3188.
- Jones, A. (1978). A graphics model building and refinement system for macromolecules. *J. Appl. Crystallogr.* **11**, 268–272.
- Jones, A. (1982). Frodo: a graphics fitting program for macromolecules. In *Computational Crystallography* (Sayre, D., ed.), pp. 303–317, Oxford University Press, Oxford.
- Jones, T. A. (1985). Interactive computer graphics: FRODO. *Methods Enzymol.* **115**, 157–171.
- Jones, T. A., Bergdoll, M. & Kjeldgaard, M. (1990). O: a macromolecule modeling environment. In *Crystallographic and Modeling Methods in Molecular Design* (Bugg, C. & Ealick, S., eds), pp. 189–199, Springer-Verlag, New York.
- Kallis, G.-B. & Holmgren, A. (1980). Differential reactivity of the functional sylphydryl groups of cysteine-32 and cysteine-35 present in the reduced form of thioredoxin from *Escherichia coli*. *J. Biol. Chem.* **255**, 10261–10265.
- Karplus, P. A. & Schulz, G. E. (1987). Refined structure of glutathione reductase at 1.54 Å resolution. *J. Mol. Biol.* **195**, 701–729.
- Katti, S. K., LeMaster, D. M. & Eklund, H. (1990). Crystal structure of thioredoxin from *Escherichia coli* at 1.68 Å resolution. *J. Mol. Biol.* **212**, 167–184.
- Kraulis, P. J. (1991). MOLSCRIPT: a program to produce both detailed and schematic plots of protein structures. *J. Appl. Crystallogr.* **24**, 946–950.
- Ladenstein, R., Epp, O., Bartels, K., Jones, A., Huber, R. & Wendel, A. (1979). Structure analysis and molecular model of the selenoenzyme glutathione peroxidase at 2.8 Å resolution. *J. Mol. Biol.* **134**, 199–218.
- Laurent, T. C., Moore, E. C. & Reichard, P. (1964). Enzymatic synthesis of deoxyribonucleotides. IV. Isolation and characterization of thioredoxin, the hydrogen donor from *Escherichia coli* B. *J. Biol. Chem.* **239**, 3436–3444.
- Lee, B. K. & Richards, F. M. (1971). The interpretation of protein structures: estimation of static accessibility. *J. Mol. Biol.* **55**, 379–400.
- LeMaster, D. M. & Richards, F. M. (1988). NMR sequential assignment of *Escherichia coli* thioredoxin utilizing random fractional deuteration. *Biochemistry*, **27**, 142–150.
- Levitt, M. & Chothia, C. (1976). Structural patterns in globular proteins. *Nature (London)*, **261**, 552–558.
- Lewis, S. D., Johnson, F. A. & Shafer, J. A. (1976). Potentiometric determination of ionizations at the active site of papain. *Biochemistry*, **15**, 5009–5017.
- Mattevi, A., Schierbeek, A. J. & Hol, W. G. J. (1991). Refined crystal structure of lipoamide dehydrogenase from *Azotobacter vinelandii* at 2.2 Å resolution. *J. Mol. Biol.* **220**, 975–994.
- Matthews, B. W. (1968). Solvent content of protein crystals. *J. Mol. Biol.* **33**, 491–497.
- Nikkola, M., Gleason, F., Saarinen, M., Joelson, T., Björnberg, O. & Eklund, H. (1991). A putative gluta-

- thione binding site in T4 glutaredoxin investigated by site-directed mutagenesis. *J. Biol. Chem.* **266**, 16105–16112.
- Nilsson, O. (1991). Molecular dynamics modelling of bacteriophage T4 glutaredoxin. Thesis, University of Stockholm, Sweden.
- Nilsson, O., Tapia, O. & van Gunsteren, W. F. (1990). Structure and fluctuations of bacteriophage T4 glutaredoxin modelled by molecular dynamics. *Biochem. Biophys. Res. Commun.* **171**, 581–588.
- Nyborg, J. & Wonacott, A. J. (1977). Computer programs. In *The Rotation Method in Crystallography* (Arndt, U. W. & Wonacott, A. J., eds), pp. 139–152, North Holland Publishing Co., Amsterdam.
- Reinemeyer, P., Dirr, H. W., Ladenstein, R., Schäffer, J., Gallay, O. & Huber, R. (1991). The three-dimensional structure of class  $\pi$  glutathione S-transferase in complex with glutathione sulfonate at 2.3 Å resolution. *EMBO J.* **10**, 1997–2005.
- Richardson, J. S. (1977).  $\beta$ -Sheet topology and the relatedness of proteins. *Nature (London)*, **268**, 495–500.
- Richardson, J. S. (1981). The anatomy and taxonomy of protein structure. *Advan. Protein Chem.* **34**, 167–339.
- Sandberg, V., Kren, B., Fuchs, J. A. & Woodward, C. (1991). *Escherichia coli* glutaredoxin: cloning and overexpression, thermodynamic stability of the oxidized and reduced forms, and report of an N-terminal extended species. *Biochemistry*, **30**, 5475–5484.
- Schellman, C. (1980). The  $\alpha L$  conformation at the ends of helices. In *Protein Folding* (Jaenick, R., ed.), pp. 53–61, Elsevier, Amsterdam.
- Schiering, N., Kabsch, W., Moore, M. J., Distefano, M. D., Walsh, C. T. & Pai, E. F. (1991). Structure of the detoxification catalyst mercuric ion reductase from *Bacillus* sp. strain-RC607. *Nature (London)*, **352**, 168–172.
- Sjöberg, B.-M. & Söderberg, B.-O. (1976). Thioredoxin induced by bacteriophage T4: crystallization and preliminary crystallographic data. *J. Mol. Biol.* **100**, 415–419.
- Smith, J. L., Hendrickson, W. A., Honzatko, R. B. & Sheriff, S. (1986). Structural heterogeneity in protein crystals. *Biochemistry*, **25**, 5018–5027.
- Sodano, P., Xia, T. H., Bushweller, J. H., Björnberg, O., Holmgren, A., Billeter, M. & Wüthrich, K. (1991). Sequence-specific H-1 n.m.r. assignments and determination of the three-dimensional structure of reduced *Escherichia coli* glutaredoxin. *J. Mol. Biol.* **221**, 1311–1324.
- Söderberg, B.-O., Sjöberg, B.-M., Sonnerstam, U. & Brändén, C.-I. (1978). Three-dimensional structure of thioredoxin induced by bacteriophage T4. *Proc. Nat. Acad. Sci., U.S.A.* **75**, 5827–5830.
- Sussmann, J. L., Holbrook, S. R., Church, G. M. & Kim, S.-H. (1977). A structure-factor least-squares refinement procedure for macromolecular structures using constrained and restrained parameters. *Acta Crystallogr. sect. A*, **33**, 800–804.
- Thornton, J. M. (1981). Disulphide bridges in globular proteins. *J. Mol. Biol.* **151**, 261–287.
- Tickle, I. J. (1985). Review of space group general translation functions that make use of known structural information and can be expanded as Fourier series. In *Molecular Replacement* (Machin, P. A., ed.), pp. 22–26, Science & Engineering Research Council, Daresbury, England.

Edited by R. Huber